Charge Self-Consistent Empirical Tight-Binding Cluster Method for Semiconductor Surface Structures

by

Jonathan Neil Carter.

A thesis submitted to the

University of Warwick

for admission to the degree of

Doctor of Philosophy.

Department of Physics.

September 1988.

Contents

List of Figures

List of Tables

Acknowledgements.

I would like to take this opportunity to thank some of the many people who have helped me reach the point where I am able to submit this thesis:-

- My parents and family for the support they have given to me over the years of my academic career;
- Dr B.W. Holland for his guidance, and for pointing me in the right direction each time I forgot the aim of the research;
- Dr V. Dwyer, Mr M. Kearney and Mr A. Wander for taking the time and effort to explain things to me;
- Dr P.V. Smith for his critical reading of this thesis;
- My colleagues at Warwick for their friendship;
- The Department of Physics for the provision of facilities and SERC for financial support and the provision of computer resources;
- The staff of Warwick University Computer Services, in particular Mr J. Hicks for his assistance, and the staff of UMRCC and ULCC;
- Finally Ms Rona Tan for helping me type this thesis.

Declaration.

This thesis (written in accordance with PHYS/PG3) contains an account of my own research (except the work presented in section 5.2.1 and the self-consistent result for the Si(111)(2x1) surface in table 5.1, which was performed by Dr V.M. Dwyer) carried out in the Department of Physics at the University of Warwick, between October 1985 and August 1988, under the general supervision of Dr B.W. Holland.

No part of this work has been previously submitted to this or any other academic institution for admission to a higher degree. Some parts of it have already been published, and are as follows:

- Empirical Tight-Binding Cluster Method for Semiconductor Surface Structures,
  J.N. Carter, V.M. Dwyer and B.W. Holland.
  Surface Science 188, L723, 1987.

- Charge Self-Consistent Empirical Tight-Binding Cluster Method for Semiconductor Surface Structures,
  V.M. Dwyer, J.N. Carter and B.W. Holland.
  Proceedings of the Second International Conference on the Structure of Surfaces, Springer Series in Surface Sciences, 11, 320, 1988. Editors J.F. van der Veen and M.A. Van Hove.

- Structure of the α phase of Ge(111)$\sqrt{3}$x$\sqrt{3}$-Pb,
  J.N. Carter, V.M. Dwyer and B.W. Holland.
  Solid State Communications, 67, 643, 1988.

It is hoped to publish the work in chapter 7 on the (100) surface of Cubic Silicon Carbide in the near future.

J.N Carter

J.N. Carter

Abstract.

In this thesis a cluster method for evaluating the structure of semiconductor surfaces is formulated. Chadi's total energy algorithm is used to express the total energy of a cluster in terms of a sum of one-electron energies and a residual energy term. The one-electron energies are calculated within Harrison's Tight-Binding Approximation, using his empirical interatomic matrix elements. The residual energy, being the difference between the ion-ion and electron-electron interaction energies, is treated as a bond stretching energy summed over all bonds in the cluster. The energy of a bond is evaluated by comparison with the change in energy as a function of bond length as determined by a quantum chemistry calculation. A cluster includes all the atoms that are expected to be displaced from their bulk positions and enough other atoms such that displaced atoms have the correct local bonding. The edge of the cluster is saturated with Hydrogen atoms. A form of self-consistency is included by relating the distribution of charge to changes in the atomic term values and iterating the process until self-consistency is achieved. The model is tested on the Si(111)(2x1), Si(100)(2x1) and GaAs(110)(1x1) surfaces, and then used for calculations on the Ge(111) and β-SiC(100) surfaces.

Abbreviations.

AES	Auger Electron Spectroscopy
BCC	Body Centred Cubic
CVD	Chemical Vapour Deposition
ETBM	Empirical Tight-Binding Method
FCC	Face Centred Cubic
LCAO	Linear Combination of Atomic Orbitals
LEED	Low Energy Electron Diffraction
MBE	Molecular Beam Epitaxy
NSC	Non-Self-Consistent
SC	Self-Consistent
SERC	Science and Engineering Research Council
SEXAFS	Surface Extended X-ray Absorption Fine Structure
SXD	Surface X-ray Diffraction
UHV	Ultra-High Vacuum
ULCC	University of London Computer Centre
UMRCC	University of Manchester Regional Computer Centre

"There is no such thing as a problem without a gift for you in its hands.

You seek problems because you need their gifts."

— Richard Bach, Illusions.

Chapter 1

Motivation and Preview.

"Begin at the beginning", the king said, gravely, "and, go on till you come to the end: then stop."

— Lewis Carroll, Alice in Wonderland.

1.1 Motivation.

The advances that have been made in the last decade in the fabrication of solid-state devices have been dramatic, with the scale of the devices becoming such that their behaviour is beginning to depend on surface and interface effects. Also there has been the development of Molecular Beam Epitaxy (MBE) to the point where devices of one or two monolayers can be put down (Sano et al., 1984), in such devices it is important to know how the surface grows. To understand both surface and interface effects it is necessary to know the electronic structure involved, this is directly dependent on the atomic structure found (which may be very different from that to be found in the bulk crystal).

The experimental study of surfaces has developed mainly in the last twenty-five years with the development of ultra-high vacuum technology (UHV), there now exists a wide range of surface sensitive techniques available including: Low Energy Electron Diffraction (LEED), Auger Electron Spectroscopy (AES) and Surface Extended X-ray Absorption Fine Structure (SEXAFS). For an extensive guide to the properties of surfaces and the techniques for studying them one should consult books by Zangwill (1988), Woodruff and Delchar (1986).

From a theoretical point of view, without reference to experimental data, about the only option available to determine surface structure is some form of total energy minimisation. Attempts to do this with respect to the structural parameters of the surface have generally followed one of two approaches. The "Solid-state" approach (Chadi, 1978; Pandey, 1982), in which Bloch's theorem plays a central role, and which cannot treat non-periodic defects; or the "Chemical" approach (Swarts, 1981; Barone, 1985) in which the surface is represented by a small atomic cluster on which the sophisticated methods of quantum chemistry are used. Both methods obtain results which are comparable to experiment.

The principle difficulty with the quantum chemistry methods is that they can only treat small clusters of atoms, because of the excessive demands made on computer time. The same problem exists for the solid-state approach when first-principle self-consistent methods are used (Pandey, 1982). Chadi (1978) has shown that valuable results can be obtained when using an empirical tight-binding model within the solid-state approach. The aim of the work presented in this thesis is to develop a model similar to that proposed by Chadi and apply it to atomic clusters, there by obtaining a significant computational advantage over the solid-state and

chemical approaches.

1.2 Preview.

In chapters 2-5 the aim is to develop a tight-binding model that can be applied to atomic clusters to give reasonable predictions of the atomic structure of semiconductor surfaces. To achieve this I started with Harrison's (1980) tight-binding model and used this within Chadi's (1978) total energy algorithm. This then allows one to develop a consistent methodology for the construction and enlargement of atomic clusters to mimic the behaviour of the crystal surface. In this thesis I have outlined the necessary theory developed by other authors and then applied this to the clusters. Chapters 6 and 7 cover some examples of the methods application to semiconductor surfaces. The last chapter is a review and also looks at some points that could be examined within the model.

1.2.1 Chapter 2.

In this chapter the aim is to examine the ground on which Harrison's (1980) tight-binding model is built. This starts by outlining how to construct the one-electron wave function of a polyatomic system. This leads directly to the calculation of the band-structure of a periodic crystal. At this point some of the ideas of tight-binding models are introduced. The one-electron wave function is expressed as a linear combination of atomic orbitals (LCAO). When calculating the band-structure, the overlap between atomic orbitals on different atoms is ignored. Only interactions between atomic orbitals on nearest-neighbour atoms are

included. The LCAO band-structure is "fitted" to the band-structure determined by more accurate methods to determine the matrix elements which represent the nearest-neighbour interactions. Next is introduced Harrison's discovery that these parameters scale from material to material in a predictable way. The chapter concludes with a brief examination of the work that has been done to support the assumptions used within the model.

1.2.2 Chapter 3.

In this chapter the intention is to develop a particular model for the total energy of a cluster of atoms. The aim of the work that follows in later chapters is to find the minimum of this total energy with respect to "some" structural parameters that describe the cluster. We use a total energy algorithm introduced by Chadi (1978), in which the total energy is split into two terms; a sum of one-electron energies and a residual energy term. The residual energy accounts for the double counting of some energy terms in the one-electron energies and those terms not included in it. The residual energy is expressed as a bond stretching energy. The rest of the chapter considers how this algorithm is to be applied to clusters, using Harrison's tight-binding model for the one-electron energies and a quantum chemistry package to help calculate the bond stretching energy term.

1.2.3 Chapter 4.

Having a way of calculating the total energy of a given cluster, attention is now turned to how to construct a cluster so that it mimics the behaviour of an infinite periodic system. Fortunately it appears that bonding within a covalent system is

a highly localised effect, and as such, a small cluster has a very similar electronic structure to an infinite surface. The work starts by examining the cluster needed to represent a single unit cell on the surface. There then follows a consideration of how to treat the unwanted surfaces (pseudo-surfaces) which exist only because we are using a cluster and not a semi-infinite solid. The chapter concludes by looking at how to systematically extend the cluster. The accuracy of the predictions are then compared to the results obtained for different cluster sizes and for different surfaces with those of other authors.

1.2.4 Chapter 5.

In developing the model so far, one important point has been ignored. It is that the energy levels used to calculate the sum of one-electron energies are dependent on the charge distribution in the cluster, and the charge distribution is dependent on which one-electron energy levels are occupied. It is clearly desirable to calculate the one-electron energies in a self-consistent manner. The tight-binding model being adjusted in an iterative manner until self-consistency is achieved. To account for the self-consistency, the atomic term values used in the one-electron Hamiltonian are changed at each iteration in the way prescribed by Harrison (1985). This involves the charge of the atom under consideration and the Coulomb potential due to the infinite periodic array of charge produced on the surface. Also considered is an ad hoc method which discriminates against a build up of charge on a particular atom, which is the main effect seen in the non-self-consistent calculations. Both methods are compared against results produced by other means.

1.2.5 Chapter 6.

This work represents the first attempt to use the method in a regime where there are no previous calculations to compare with. It has been shown by a number of researchers, that for low coverages of Lead on the Germanium (111) surface there exist two differing phases, each with a $\sqrt{3}x\sqrt{3}R30^{\circ}$ reconstruction pattern, but at different coverages. It has been agreed that the first of these phases has a single Lead atom per unit cell and that it appears to occupy a high symmetry site. The aim of the work was to determine which of the three possible sites had the lowest energy and the positions of the atoms within the unit cell. The results are compared with the predictions obtained from the analysis of Surface X-ray Diffraction work.

1.2.6 Chapter 7.

This chapter deals with a surface for which there is much greater uncertainty and less experimental work. The surface in question is the (100) surface of Cubic Silicon Carbide. Starting from the as received samples with a surface coating of Silicon Dioxide, a sequence of different LEED patterns are seen as the surface is annealed. The aim of the work was to examine some of the possible structural models for the surface and to predict which are possible models based on the energy of each of the systems and the charge distributions found in the minimum energy configurations.

1.2.7 Chapter 8.

The thesis finishes with a review of the conclusions reached and the results obtained. The chapter also contains a consideration of problems to which the model might be applied and possible variations to its formulation that might be considered within the model.

Chapter 2

Tight-Binding Model.

"To accept the arguments of science, is to voluntarily accept other peoples errors."

— Alexander Solzhenitsyn, Cancer Ward.

2.1 Historical Development.

The forerunner of the Empirical Tight-Binding Method (ETBM) known as the Linear Combination of Atomic Orbitals (LCAO) method first saw the light of day in a paper by Bloch (1928) in which he proposed a method to solve the problem of a set of N atoms at the vertices of an N-sided regular polygon. The basic idea was to use a linear combination of the atomic orbitals of the atoms in the ring to approximate the complete wave function. For a ring of 'N' atoms with separation 'a' it can be shown that

$$\Psi(x) = U_k(x)\exp(i2\pi sx/Na) \tag{2.1}$$

(Kittel, 1976, p190) where

$$s \in \{0 \ldots N-1\}, \tag{2.2}$$

provided that $U_b(x) = U_b(x+a)$. Such a function is given by the sum of the atomic orbitals of one type of all the atoms in the ring. If we take a linear combination of all the orbitals on all the atoms, we get

$$\Psi(x) = \sum_n \phi_n(x) \exp(i2\pi sx/Na). \tag{2.3}$$

From a ring of identical atoms it is easy to generalise to an infinite chain of atoms, and hence to 3D crystals. This work underlies much of the work on the quantum theory of solids.

While the basic idea is easily carried over to solids, there are however a large number of very difficult integrals to be calculated which made the method nearly impossible to do with complete rigour. Given these points Slater and Koster (1954) proposed that the LCAO method should be used "not as a primary method of accurate calculation, but rather as an interpolation method". Their principle method of attack was to retain only those terms (matrix elements) which were required to give qualitative correctness to the method and to treat them as adjustable parameters which are fitted to the results of more accurate calculations at high symmetry points of the Brillouin zone.

With the advent of new methods and more powerful computers the need for an interpolation method diminished.

In recent years the method has been turned from an interpolation scheme for the band structure of crystalline solids, to an extrapolation scheme for amorphous solids and perturbed crystals, e.g. surfaces.

2.2 Linear Combinations of Atomic Orbitals.

In this chapter the aim is to outline the ideas behind the tight-binding model. We start here with the ideas that underlie the LCAO method.

The prime assumption that we use is that the one-electron wave function of a polyatomic system can be written as a sum of atomic basis functions

$$|\Psi_\nu(r)>=\sum_{\alpha j} F^\nu_{\alpha j}|\phi_\alpha(r-R_j)>, \tag{2.4}$$

where

- $|\Psi_\nu(r)>$ is the one-electron wave function
- $|\phi_\alpha(r-R_j)>$ is the atomic orbital $|\phi_\alpha(r)>$ on the jth atom

the sum being over all orbitals and atoms.

If we substitute equation 2.4 into the time-independent Schrödinger equation we obtain

$$\sum_{\alpha j} F^\nu_{\alpha j} H|\phi_\alpha(r-R_j)>=\sum_{\alpha j} F^\nu_{\alpha j} E^\nu|\phi_\alpha(r-R_j)>, \tag{2.5}$$

where H is the one-electron Hamiltonian and E^ν is an eigenvalue. If we now pre-multiply by $<\phi_\beta(r-R_i)|$, we obtain a series of simultaneous equations

$$\sum_{\alpha j} F^\nu_{\alpha j} H_{\beta,\alpha}(R_i-R_j)=\sum_{\alpha j} F^\nu_{\alpha j} E^\nu S_{\beta,\alpha}(R_i-R_j), \tag{2.6}$$

where

$$H_{\beta,\alpha}(R_i-R_j)=<\phi_\beta(r-R_i)|H|\phi_\alpha(r-R_j)> \tag{2.7}$$

and

$$S_{\beta,\alpha}(R_i-R_j)=<\phi_\beta(r-R_i)|\phi_\alpha(r-R_j)> \tag{2.8}$$

Equation 2.6 may be written in the form of a matrix equation

$$HF^{\nu} = E^{\nu}SF^{\nu}, \tag{2.9}$$

hence we need to solve

$$\det(H - E^{\nu}S) = 0 \tag{2.10}$$

(we may then solve for F^{ν} also).

For a crystalline solid, we may according to Bloch's theorem, write $F^{\nu}_{\alpha_j}$ in the following form

$$F^{\nu}_{\alpha_j} = C^{n}_{\alpha}(k)\exp(ik.R_j) \tag{2.11}$$

($\nu = n, k$, where n numbers the solutions for a given k), R_j being the bravais lattice sites. Equation 2.6 can now be written in the following form

$$\sum_{\alpha}\{H_{\alpha,\alpha'}(k) - E_n(k)S_{\alpha,\alpha'}(k)\}C^{n}_{\alpha}(k) = 0 \tag{2.12}$$

with

$$H_{\alpha,\alpha'}(k) = N^{-1}\sum_{j}\exp(ik.R_j)H_{\alpha,\alpha'}(R_j) \tag{2.13}$$

and

$$S_{\alpha,\alpha'}(k) = N^{-1}\sum_{j}\exp(ik.R_j)S_{\alpha,\alpha'}(R_j), \tag{2.14}$$

N being the number of lattice sites in the crystal. Equation 2.10 is now written as

$$\det(H(k) - E_n(k)S(k)) = 0. \tag{2.15}$$

Solving equation 2.15 yields the energy bands $E_n(k)$ of the crystal.

From equation 2.15 it is possible to proceed in a variety of different ways depending on what prescription one uses to evaluate equations 2.7 and 2.8. One could proceed directly and evaluate each of the terms $H_{\alpha,\alpha'}$ and $S_{\alpha,\alpha'}$, this however

becomes difficult due to the number of multicentral integrals. An alternative approach is that of the Extended Hückel Method in which it is assumed that $H_{\alpha\alpha'}$ is proportional to $S_{\alpha\alpha'}$ (α and α' are not on the same atom).

The way we proceed is that set out by Slater and Koster (1954) in which they treat the Hamiltonian elements $H_{\alpha,\alpha'}$ as parameters which are fitted to accurate calculations at high symmetry points of the Brillouin zone.

2.3 Band Structure Calculations.

Following the work of Slater and Koster (1954) a number of groups used the LCAO method as an interpolation scheme. In particular I wish to follow the work published in a paper by Chadi and Cohen (1975) which contains many of the simplifications that are used later by Harrison (1980).

Let us consider the case of diamond or zincblende crystals. Within each primative cell there are two inequivalent tetrahedrally coordinated atoms, which can be labelled 'type 1' or 'type 2'. If we have two sets of tight-binding basis functions $|\phi_\alpha^1(r-R_j)>$ and $|\phi_\alpha^2(r-R_j)>$ (R_j defines a bravais lattice centred on the atom) then from equations 2.4 and 2.11 we may construct the following Bloch functions,

$$|\Psi_\alpha^1(k,r)>= N^{-1}\sum_j \exp(ik.R_j)|\phi_\alpha^1(r-R_j)> \tag{2.16}$$

$$\cdot\ |\Psi_\alpha^2(k,r)>= N^{-1}\sum_j \exp(ik.R_j)|\phi_\alpha^2(r-R_j)>\ . \tag{2.17}$$

An assumption that can be placed on the one-electron wave functions $|\Psi_\alpha^i>$ is that they are orthonormal (this is done to simplify the computation involved), i.e.

$$<\Psi_\alpha^i(k,r)|\Psi_{\alpha'}^j(k,r)>= \delta_{ij,\alpha\alpha'}\ \forall k, \tag{2.18}$$

from equations 2.16 and 2.17 we get,

$$N^{-2}\sum_{lm}\exp(-ik.R_l)\exp(ik.R_m) < \phi^i_\alpha(r-R_l)|\phi^j_{\alpha'}(r-R_m) >= \delta_{i\alpha,j\alpha'}\ \forall k, \quad (2.19)$$

which can only be true if

$$< \phi^i_\alpha(r-R_l)|\phi^j_{\alpha'}(r-R_m) >= \delta_{i\alpha,j\alpha'}. \quad (2.20)$$

If we now assume that the orbitals $|\phi^i_\alpha>$ are in fact the atomic orbitals at each site, then equation 2.20 becomes

$$< \phi^i_\alpha|\phi^j_{\alpha'} >= S_{\alpha i,\alpha' j} = \delta_{i\alpha,j\alpha'} \quad (2.21)$$

(this assumption will be considered in section 2.5.4). Hence equation 2.15 reduces to

$$\det(H(k) - E_n(k)) = 0. \quad (2.22)$$

The basic problem is to evaluate the matrix elements $H_{\alpha i,\alpha' j}$ between the various atomic orbitals. Following Chadi (1977), let us assume that for diamond and zincblende crystals only the outermost $|S>$ and three $|P>$ orbitals are important at each site. Then the Hamiltonian can be written as an 8x8 matrix.

Let us consider now how we build the Hamiltonian by looking in detail at the matrix element between the atomic orbitals $|S^1>$ and $|S^2>$, from equation 2.13.

$$H_{S^1,S^2}(k) = N^{-1}\sum_j \exp(-ik.R_j)N^{-1}\sum_i \exp(ik.R_i) < S^1(r-R_j)|H|S^2(r-R_i) >, \quad (2.23)$$

now since the two bravais lattices defined on each of the two atom sites are separated by d', where d' is the vector joining the atoms in the unit cell. If we now relate the two bravais lattices to a single lattice by

$$R_i = R_j + d' \quad (2.24)$$

and make the following substitution (dropping the reference to the atoms, Harrison, 1980, p77)

$$E_{ss} = < S^1(r - R_j)|H|S^2(r - R_i) > \tag{2.25}$$

then the Hamiltonian element becomes

$$H_{S^1S^2}(k) = \sum_{d'} \exp(ik.d')E_{ss}(d')$$

If we now restrict the sum over d' to nearest-neighbours (this being the Tight-Binding Approximation (TBA)), then

$$H_{S^1S^2}(k) = g_1(k)E_{ss} \tag{2.26}$$

with

$$g_1(k) = \exp(ik.d_1) + \exp(ik.d_2) + \exp(ik.d_3) + \exp(ik.d_4) \tag{2.27}$$

and

$$\begin{aligned} d_1 &= (1,1,1)a/4 \\ d_2 &= (1,\bar{1},\bar{1})a/4 \\ d_3 &= (\bar{1},1,\bar{1})a/4 \\ d_4 &= (\bar{1},\bar{1},1)a/4 \end{aligned} \tag{2.28}$$

'a' is the lattice constant.

One can carry out similar calculations for each of the Hamiltonian elements, when we do this we find we need the following relationships

$$\begin{aligned} g_2(k) &= \exp(ik.d_1) + \exp(ik.d_2) - \exp(ik.d_3) - \exp(ik.d_4) \\ g_3(k) &= \exp(ik.d_1) - \exp(ik.d_2) + \exp(ik.d_3) - \exp(ik.d_4) \\ g_4(k) &= \exp(ik.d_1) - \exp(ik.d_2) - \exp(ik.d_3) + \exp(ik.d_4) \end{aligned} \tag{2.29}$$

Then using the fact that the Hamiltonian Matrix is hermitian we can write down the matrix given in table 2.1. The elements down the leading diagonal are known

	S^1	S^2	P^1_x	P^1_y	P^1_z	P^2_x	P^2_y	P^2_z
S^1	ϵ^1_s	$E_{ss}g_1$	0	0	0	$E_{sp}g_2$	$E_{sp}g_3$	$E_{sp}g_4$
S^2	$E_{ss}g_1^*$	ϵ^2_s	$-E_{sp}g_2^*$	$-E_{sp}g_3^*$	$-E_{sp}g_4^*$	0	0	0
P^1_x	0	$-E_{sp}g_2$	ϵ^1_p	0	0	$E_{xx}g_1$	$E_{xy}g_4$	$E_{xz}g_3$
P^1_y	0	$-E_{sp}g_3$	0	ϵ^1_p	0	$E_{xy}g_4$	$E_{yy}g_1$	$E_{yz}g_2$
P^1_z	0	$-E_{sp}g_4$	0	0	ϵ^1_p	$E_{xz}g_3$	$E_{yz}g_2$	$E_{zz}g_1$
P^2_x	$E_{sp}g_2^*$	0	$E_{xx}g_1^*$	$E_{xy}g_4^*$	$E_{xz}g_3^*$	ϵ^2_p	0	0
P^2_y	$E_{sp}g_3^*$	0	$E_{xy}g_4^*$	$E_{yy}g_1^*$	$E_{yz}g_2^*$	0	ϵ^2_p	0
P^2_z	$E_{sp}g_4^*$	0	$E_{xz}g_3^*$	$E_{yz}g_2^*$	$E_{zz}g_1^*$	0	0	ϵ^2_p

Table 2.1: Tight-binding Hamiltonian for the Zincblende structure.

as atomic term values.

We are now in a position to evaluate the energy bands as a function of k by diagonalising the Hamiltonian. If we choose suitable values for the atomic term values, e.g. those used by Harrison (1980), then we can adjust the parameters E_{ss} etc to fit the tight-binding energy bands to those calculated by a more accurate method at a selection of high symmetry points within the Brillouin zone.

Figure 2.1 compares some tight-binding results obtained by Harrison (1980) for Germanium with the bands obtained by Grobman et al. (1975) who used a combination of pseudopotential calculations and experiment.

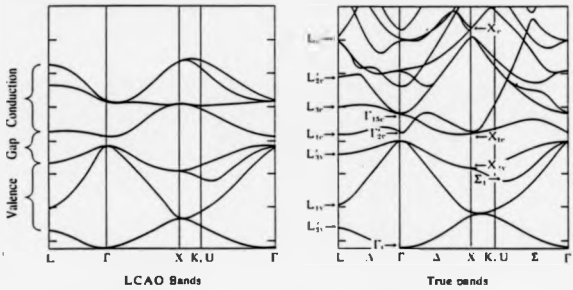

Figure 2.1: Comparison of some tight-binding bands with those produced using pseudopotentials for Germanium (Harrison, 1980; Grobman et al., 1975).

2.4 Harrison's Universal Parameters.

We have now specified the basic assumptions and methods used within the tight-binding model,

- use of $|S>$ and $|P>$ orbitals only
- nearest-neighbour interactions only to be included
- orthogonality of atomic basis functions
- use of atomic term values
- fitting of the LCAO bands to accurate calculations using the parameters E_{ss} etc.

This in principle now allows us to produce a reasonable representation of the valence bands of any compound for which the above conditions hold true.

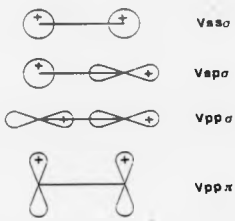

Figure 2.2: Relationship between the $|S>$ and $|P>$ orbitals on two atoms and the interatomic matrix elements.

Harrison in a series of papers (Pantelides and Harrison, 1975; Harrison, 1977; Froyen and Harrison, 1979) used a slight variation on the method used in the previous section. Rather than use the four atomic orbitals centred on each site, he used four SP^3 hybrids. Also the parameters used in the previous section E_{ss} etc, are expressed in terms of atomic orbital matrix elements, $V_{ss\sigma}$ $V_{sp\sigma}$ $V_{pp\sigma}$ and $V_{pp\pi}$, as tabulated in Slater and Koster (1954). The atomic matrix elements label the matrix elements between orbitals on different atoms (see figure 2.2).

The *remarkable* discovery made in this series of papers (initially by empirical means, latterly theoretical justification was provided), was that for a tight-binding model of a covalent tetrahedrally bonded crystal using the the assumptions given above, the atomic matrix elements scaled from material to material according to a d^{-2} rule (d being the equilibrium bond length). I will outline here the theoretical justification of the scaling rule, which was first given in the third of these papers.

Figure 2.3 shows the energy bands of Germanium as calculated using an empirical non-local pseudopotential scheme (Chelikowsky and Cohen, 1976) and a

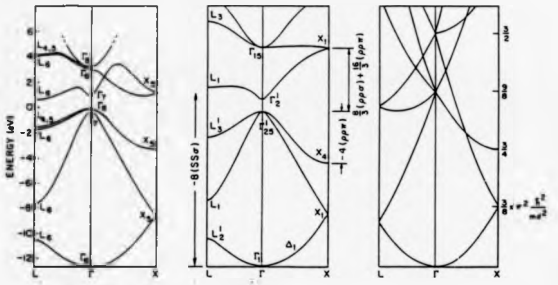

Figure 2.3: Three forms of the energy bands of Germanium calculated with a empirical-nonlocal-pseudopotential (Chelikowsky, 1976), a LCAO model (Chadi, 1976) and the free electron model.

LCAO model (Chadi and Cohen, 1975), along side the free-electron bands. The pseudopotential valence bands and the LCAO valence bands are very similar, and both have some resemblance to the free-electron bands. This suggested to Harrison that the LCAO parameters could be obtained by fitting the LCAO bands to those of the free-electron model.

To fit the six LCAO parameters Harrison chose to equate the bands at points where they appeared most similar, these are given in table 2.2. Using the points Γ_1 Γ_2' Γ_{25}' Γ_{15} and X_4 it is possible to evaluate values for V_{sss} V_{pps} and V_{ppp} which do not depend upon ϵ_s and ϵ_p (due to the arbitrary zero point for the free-electron bands), however to get the correct band gap it is necessary to use the atomic term values for ϵ_s and ϵ_p. Since V_{spp} depends on these values it is useful to determine it in a different way. This is done by setting the "effective mass at the bottom of the

Point	LCAO	Free-electron
Γ_1	$\epsilon_s + 4V_{ss\sigma}$	0
Γ_2'	$\epsilon_s - 4V_{ss\sigma}$	$\frac{2\pi^2}{6}\frac{\hbar^2}{m_e a^2}$
Γ_{25}'	$\epsilon_p - \frac{4}{3}V_{pp\sigma} - \frac{8}{3}V_{pp\pi}$	$\frac{2\pi^2}{6}\frac{\hbar^2}{m_e a^2}$
Γ_{15}	$\epsilon_p + \frac{4}{3}V_{pp\sigma} + \frac{8}{3}V_{pp\pi}$	$\frac{2\pi^2}{2}\frac{\hbar^2}{m_e a^2}$
X_1	$\frac{\epsilon_s+\epsilon_p}{2} - \left[\left(\frac{\epsilon_p-\epsilon_s}{2}\right)^2 + \frac{16}{3}V_{sp\sigma}^2\right]^{1/2}$	$\frac{2\pi^2}{8}\frac{\hbar^2}{m_e a^2}$
X_4	$\epsilon_p - \frac{4}{3}V_{pp\sigma} + \frac{4}{3}V_{pp\pi}$	$\frac{2\pi^2}{4}\frac{\hbar^2}{m_e a^2}$

Table 2.2: Expressions for LCAO and free-electron band energies (Froyen and Harrison, 1979).

$V_{ss\sigma}$	$-\frac{9\pi^2}{64}\frac{\hbar^2}{m_e a^2}$
$V_{sp\sigma}$	$\frac{9\pi^2}{32}\left(1-\frac{16}{3\pi^2}\right)^{1/2}\frac{\hbar^2}{m_e a^2}$
$V_{pp\sigma}$	$\frac{21\pi^2}{64}\frac{\hbar^2}{m_e a^2}$
$V_{pp\pi}$	$-\frac{3\pi^2}{32}\frac{\hbar^2}{m_e a^2}$

Table 2.3: Analytical expressions for the Universal Parameters (Froyen and Harrison, 1979).

'S' band equal to the free-electron mass" (for the details see Froyen and Harrison, 1979).The values obtained by Froyen and Harrison are given in table 2.3. Using exactly this approach it was possible to evaluate appropriate parameters for other structures (simple cubic, FCC, BCC).

It is these "universal parameters" that we will be using in later calculations.

2.5 Critique of Harrison's Tight-Binding Model.

In this section I wish to examine in greater detail some of the work that supports the main assumptions within tight-binding models in general and Harrison's model in particular, the assumptions being: the need for $|S>$ and $|P>$ orbitals only, nearest-neighbour interactions only, the scaling rule for the universal parameters and the orthogonality of the basis set.

For a more general critique of tight-binding methods for semi-conductors one should read Pantelides and Pollmann (1979).

2.5.1 Size of Basis Set.

To examine the question as to how large the basis set needs to be it is useful not to work within a tight-binding model, but to use a more accurate technique. This was done by Chadi (1977) when he used an empirical pseudopotential Hamiltonian to predict the band-structure of Silicon, Germanium and Gallium Arsenide.

He considered two cases, the first involved four basis functions (one $|S>$ and three $|P>$) per site, the second had five additional $|d>$ orbitals and one "f-like" orbital. In figure 2.4 are the results for Germanium using four basis functions compared to the exact results obtained by Cohen and Bergstresser (1966).

Chadi made the following conclusion:

> "We have shown that a simple basis set consisting of $|S>$ and $|P>$ orbitals can give an accurate description of the valence and conduction band-structures of diamond and zincblende semiconductors. For accurate energy bands *and* wave functions we find a ten state per atom

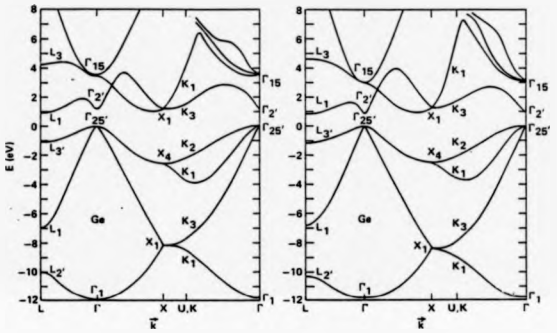

Figure 2.4: Comparison of the energy bands for Germanium using a LCAO four orbital model (Chadi, 1977) and the exact bands obtained by Cohen and Bergstresser (1966).

basis that includes $|d>$ orbitals to be sufficient for the valence and the first few conduction bands."

Since we will be only interested in the valence bands, the $|S>$ and $|P>$ basis set should be adequate for our purposes.

2.5.2 Nearest-Neighbour Interactions.

While it is true that the eigenstates of a covalently bonded crystal are not confined to a particular region, it is found however that the amplitude of the wave function is of significance only in a fairly small region. Therefore one only needs to include interactions within a limited area.

The question as to which interactions should be included is most often decided by the accuracy that is required for the valence bands, it is unusual for more than second nearest-neighbour interactions to be included (see Chadi and Cohen, 1975).

In their paper Pantelides and Pollmann (1979) offer the following exposition of the Tight-Binding Approximation. Consider a simple linear chain of atoms with atomic spacing 'a', then equation 2.13 may be written as

$$H_{\alpha\alpha'}(k) = V_1 \cos(ka) + \sum_{n\neq 1} V_n \cos(nka) \tag{2.30}$$

where

$$V_n = H_{\alpha\alpha'}(R_j) \qquad \text{j = nth neighbour shell} \tag{2.31}$$

If we define

$$\lambda(k) = 1 + \sum_{n\neq 1} \left(\frac{V_n}{V_1} \frac{\cos(nka)}{\cos(ka)} \right) \tag{2.32}$$

then we may write

$$H_{\alpha\alpha'} = \lambda(k) V_1 \cos(ka) \tag{2.33}$$

if we compare this to the tight-binding equivalent (c.f. equation 2.26)

$$H_{\alpha\alpha'} = V\cos(ka) \tag{2.34}$$

one can see that the tight-binding model replaces $\lambda(k)V_1$ with its average over the Brillouin zone. This argument can clearly be extended from infinite chains to 3D crystals.

2.5.3 Scaling Rule for the Universal Parameters.

Harrison's d^{-2} scaling rule was established by examining how the interatomic matrix elements scaled from material to material. As pointed out by Smith (1986), "the real question ... is whether this d^{-2} ansatz correctly describes the way in which the LCAO interatomic matrix elements of a given covalent solid vary with interatomic spacing."

In a series of papers (Smith and McMahon, 1983; Robertson, 1983; Smith, 1985, 1986) the tight-binding parameters were fitted to pressure dependent pseudopotential band-structures. Then the variation of the parameters was compared to those predicted by the d^{-2} scaling rule, it transpires that the d^{-2} scaling rule always under-estimates the variations. Smith (1985, 1986) also checked some of the predictions for bulk properties made by Chadi (1978) (this is of much greater importance from the position of the work presented in this thesis, because in later chapters we will be using what is essentially Chadi's total energy model). In table 2.4 are the values produced by Smith (1986) for the elastic constants and of the Γ and X point phonon frequencies of Silicon.

Quoting from Smith's (1986) results:

Elastic Property	Experimental Values (from a variety of sources)	Model	
		$\frac{1}{d^2}$ Scaling	Pseudopotential Hamiltonian
$C_{11} - C_{12}$ (10^{11} erg/cm^3)	10.18, 10.21	8.52	8.56
C_{44} (10^{11} erg/cm^3)	7.96	8.25	8.22
$\omega_{TA}(X)$ (THz)	4.35, 4.49	5.20	5.12
$\omega_{TA}(L)$ (THz)	3.43	4.12	4.04
$\omega_{TO}(\Gamma)$ (THz)	15.5, 15.3	17.3	14.8
$\omega_{TO}(X)$ (THz)	13.9, 14.2	14.9	14.8
$\omega_{LAO}(X)$ (THz)	11.9, 12.3	13.1	12.2
$\omega_{TO}(L)$ (THz)	14.7	16.2	15.8
$\omega_{LO}(L)$ (THz)	12.6	11.6	10.5
$\omega_{LA}(L)$ (THz)	11.4	13.2	11.0

Table 2.4: Comparison of d^{-2} scaling and a pseudopotential Hamiltonian (from Smith 1986).

> "Probably the most significant feature of the results ... is the good agreement between the predictions of both models and the experimental values, for all of the lattice dynamical properties studied. Such observations are important in establishing the overall validity and usefulness of the Chadi total energy algorithm", see chapter 3, "and in justifying its extension to the determination of the various surface geometries of these covalent solids. Moreover, they establish that suf-

ficient compensation always occurs within the Chadi total energy algorithm between the band-structure contribution, E_{BS}, and the short range force term, U, to result in values which are relatively insensitive to the choice of spatial model."

What would be particularly useful would be the repetition of Chadi's surface calculations but using a Hamiltonian fitted to the pressure dependent pseudopotential band structure. However at this time such calculations have not been performed.

2.5.4 Orthogonality of the Basis Set.

When we developed the tight-binding model of the band-structure in section 2.3, it was necessary to assume that all the atomic orbitals were orthonormal (equation 2.21), this assumption is clearly untrue. The point was resolved in a paper by Löwdin (1950). I shall present here the case for molecular orbitals which will be needed in later chapters. For the Bloch orbitals that were used in section 2.3 arguments very similar to those given below apply to give the same final result, however I will not deal with the details here.

For molecular orbitals we have (equation 2.9)

$$HF^{\nu} = E^{\nu}SF^{\nu}, \tag{2.35}$$

and from equations 2.4, 2.8 and 2.18 we get

$$F^{*\nu}SF^{\nu} = 1 \tag{2.36}$$

(where $F^{*\nu}$ is the complex conjugate of F^{ν}).

Let us define

$$F^{\nu} = S^{-1/2}C^{\nu} \tag{2.37}$$

(where $S^{-1/2}$ is some matrix such that $S^{-1/2}S^{-1/2} = S^{-1}$), substituting this into equation 2.9, we have

$$H'C^{\nu} = C^{\nu}E^{\nu}, \tag{2.38}$$

with

$$H' = S^{-1/2}HS^{-1/2}. \tag{2.39}$$

We therefore need to solve

$$\det(H' - E) = 0 \tag{2.40}$$

which has the same form as equation 2.22.

Quoting from Löwdin's paper:

> "The problem of solving the secular equations including the overlap integrals $S_{\mu\nu}$ can be reduced to the same form as it has in the simplified theory (S neglected) if the matrix H is replaced with the matrix H'."

Since the Hamiltonian matrix elements are determined empirically they can be considered to be the elements of H' rather than H.

What we have done here is to take the original localised basis set and replace it with a orthogonal basis set which is a linear combination of the original basis set . In doing this the new basis set tends to be less localised than the orbitals with which we started.

Chapter 3

Evaluation of the Total Energy.

"In these days, a man who says a thing cannot be done is quite apt to be interrupted by some idiot doing it."

— Elbert Hubbard.

3.1 Introduction.

The aim of the work is to minimise the total energy with respect to the structural parameters of a particular cluster of atoms, which are intended to approximate to a crystal surface. For a specific cluster the total energy is calculated using a sum of one-electron energies and a parameterized form for the residual energy.

The total energy of an electron-ion system can be written as the sum of four terms:

$$E_T = E_{KE} + E_{ie} + E_{ee} + E_{ii}, \tag{3.1}$$

- E_{KE} is the electron kinetic energy term,
- E_{ie} is the ion-electron interaction energy,

- E_{ee} is the electron-electron interaction energy,
- E_{ii} is the ion-ion interaction energy.

Let us first consider the information contained within a sum of one-electron energies. In particular it can be shown that within the Hartree-Fock method (see appendix A) that;

$$\sum_i \epsilon_i = E_{KE} + E_{ie} + 2E_{ee} \tag{3.2}$$

(where $\sum_i \epsilon_i$ signifies the sum over occupied one-electron states of the occupancy of the state multiplied by its energy). If we define

$$U = E_{ii} - E_{ee}, \tag{3.3}$$

then the total energy can be written in the form,

$$E_T = \sum_i \epsilon_i + U. \tag{3.4}$$

The $\sum_i \epsilon_i$ term will be calculated within Harrison's (1980) tight-binding model. Following Chadi (1978) we note: "that for ions that are separated by a distance much larger than the Thomas-Fermi screening length the combined ion-plus-screening-electron system is nearly neutral and U is close to zero. One would therefore expect that to a good approximation this term can be described by a short-range-force-constant model."

Like Chadi we will treat U as a bond stretching energy, which is expressed as a polynomial expanded about the equilibrium bond length,

$$U = \sum_{i<j} \sum_n U_n \epsilon_{ij}^n \tag{3.5}$$

where

- d_{ij} is the distance between atoms 'i', and'j',
- d_{ij}^0 is the equilibrium bond length between atoms 'i' and 'j',
- $\epsilon_{ij} = (d_{ij} - d_{ij}^0)/d_{ij}^0$.

3.2 Sum of One-electron Energies.

The basic assumptions which underlie Harrison's tight-binding model (nearest-neighbour interactions, $|S>$ and $|P>$ orbitals only and a $1/d^2$ dependence of the matrix elements) remain unchanged when we move from a bulk calculation to a surface. What one might expect to change are the parameters V_{sss}, V_{sps}, V_{pps} and $V_{ppπ}$. The assumption that is normally made is that these parameters are equally suitable for calculations on the surface or in the bulk. The justification for this comes from the use of the LCAO method to calculate surface electronic properties, when exactly this assumption is utilized (Pantelides, 1977), and the very good agreement with self-consistent pseudo-potential calculations obtained is used to justify the assumption.

Let us now consider how to construct the Hamiltonian using Harrison's prescription, which will give the required one-electron energies, for a cluster. In the case of a tetrahedrally bonded covalent solid, each atom in the equilibrium bulk state has four bonds, which are equally spaced about the atom. If we take a linear combination of the outermost $|S>$ and three $|P>$ orbitals on a particular atom, we can construct four orthonormal wave functions which have their probability

distributions pointing in the directions of the bonds, i.e.

$$
\begin{aligned}
|h_1> &= \frac{1}{2}\{|S> + |P_x> + |P_y> + |P_z>\} \text{ with direction } [111], \\
|h_2> &= \frac{1}{2}\{|S> + |P_x> - |P_y> - |P_z>\} \text{ with direction } [1\bar{1}\bar{1}], \\
|h_3> &= \frac{1}{2}\{|S> - |P_x> + |P_y> - |P_z>\} \text{ with direction } [\bar{1}1\bar{1}], \\
|h_4> &= \frac{1}{2}\{|S> - |P_x> - |P_y> + |P_z>\} \text{ with direction } [\bar{1}\bar{1}1].
\end{aligned}
\tag{3.6}
$$

We are justified in doing this, since taking linear combinations of atomic orbitals is equivalent to doing a unitary transformation on the Hamiltonian matrix. It is easy to show that these hybrids are orthonormal, $< h_i|h_j >= \delta_{ij}$ (since the $|S>$ and $|P>$ orbitals on a single atom are orthonormal).

Any rigid rotation of this set of wave functions will produce another orthonormal set, in particular the set with hybrids pointed in the opposite direction to those given above. For those atomic elements which require the use of the outermost $|S>$ orbital only, then there is only one hybrid which takes the form,

$$|h> = |S> . \tag{3.7}$$

If we have a cluster of atoms $\{i\}$ at positions $\{r_i\}$ and each atom within the cluster has hybrids $|h^i_\alpha>$, then we need to evaluate the Hamiltonian matrix elements $H_{\alpha i,\beta j} \equiv < h^i_\alpha|H|h^j_\beta >$. The matrix elements are split into three groups depending on the relationship of the atoms 'i' and 'j' .

If we write the hybrids in the form,

$$|h^i_\alpha> = \sum_\nu a^i_{\alpha\nu}|\phi^i_\nu>, \tag{3.8}$$

where $a^i_{\alpha\nu}$ are the coefficients, in equations 3.6 and 3.7, related to atomic orbitals

$|\phi^i_\nu>$. When $i = j$, i.e. hybrids on the same atom,

$$\begin{aligned} H_{\alpha i,\beta i} &= < h^i_\alpha | H | h^i_\beta > \\ &= \sum_\nu a^i_{\alpha\nu} a^i_{\beta\nu} < \phi^i_\nu | H | \phi^i_\nu >, \end{aligned} \tag{3.9}$$

since $< \phi^i_\nu | H | \phi^i_\zeta >= \epsilon_\nu \delta_{\nu\zeta}$, where ϵ_ν is an atomic term value,

$$\Rightarrow H_{\alpha i,\beta i} = \sum_\nu a^i_{\alpha\nu} a^i_{\beta\nu} \epsilon_\nu. \tag{3.10}$$

When 'i' and 'j' are nearest neighbour atoms, i.e. they are bonded covalently to each other, then we make use of the Slater-Koster (1954) interatomic matrix elements,

$$\begin{aligned} H_{\alpha i,\beta j} &= \sum_\nu a^i_{\alpha\nu} a^j_{\beta\nu} < \phi^i_\nu | H | \phi^j_\nu > \\ &= \sum_\nu a^i_{\alpha\nu} a^j_{\beta\nu} E_{\nu,\nu}. \end{aligned} \tag{3.11}$$

For $|S >$ and $|P >$ orbitals the Slater-Koster interatomic matrix elements are in terms of the parameters that Harrison used,

- $E_{S,S} = V_{sss}$,
- $E_{S,P_x} = -E_{P_x,S} = lV_{sps}$,
- $E_{S,P_y} = -E_{P_y,S} = mV_{sps}$,
- $E_{S,P_z} = -E_{P_z,S} = nV_{sps}$,
- $E_{P_x,P_x} = l^2 V_{pps} + (1 - l^2)V_{ppp}$,
- $E_{P_y,P_y} = m^2 V_{pps} + (1 - m^2)V_{ppp}$,
- $E_{P_z,P_z} = n^2 V_{pps} + (1 - n^2)V_{ppp}$,

- $E_{P_x,P_x} = E_{P_y,P_y} = lm(V_{pp\sigma} - V_{pp\pi})$,
- $E_{P_x,P_z} = E_{P_z,P_x} = ln(V_{pp\sigma} - V_{pp\pi})$,
- $E_{P_y,P_z} = E_{P_z,P_y} = mn(V_{pp\sigma} - V_{pp\pi})$,

l, m, n are the direction cosines of the bond between the atoms 'i' and 'j'.

In all other cases the Hamiltonian matrix element is zero, because we assume that we need include only interactions between nearest-neighbour atoms.

Having constructed the Hamiltonian one can evaluate the ordered set of eigenvalues ϵ_i, with ϵ_1 being the eigenvalue of lowest value. If the cluster has M valence electrons, then the sum of one-electron energies over occupied states is given by putting two electrons into each eigenstate starting with the one with lowest energy (ϵ_1) and proceeding up the list until all of the electrons have been placed in an eigenstate. If we have an odd number of electrons then the highest occupied eigenstate will only have one electron in it. The sum of the one-electron energies is given by

$$\sum_i \epsilon_i = 2 \sum_{i=1}^{|M/2|} \epsilon_i + (M - 2[M/2])\epsilon_{[M/2]+1}, \tag{3.12}$$

where $[P]$ is the largest integer $P' \leq P$.

3.3 Bond Stretching Energy.

In Chadi's (1978) original paper he used two conditions on the total energy to fix the coefficients U_1 and U_2 in equation 3.5. The conditions were that at the equilibrium bond length the total energy of the bulk crystal was at a minimum,

$$\left.\frac{\partial E_T}{\partial V}\right|_{d_0} = 0 \tag{3.13}$$

(V being the volume of the crystal), and that the bulk modulus is given by

$$V\frac{\partial^2 E_T}{\partial V^2}\bigg|_{d_0} = B \tag{3.14}$$

(B being the bulk modulus). Rather than following Chadi's approach of using bulk crystal properties to evaluate the various coefficients U_n in equation 3.5, we proceeded to evaluate $U(d)$ for a small molecule by using a quantum chemistry package (GAMESS, Gaussian 82) (see Mailhoit et al., 1985; Tománek and Schlüter 1986). Our reasons for doing this were twofold: some of the changes in bond length that we were experiencing (using approximate coefficients that were calculated within Harrison's Bond Orbital Approximation (Harrison 1980, 1973)) were such that we doubted the validity of using a quadratic form for $U(d)$, there is also a lack of suitable empirical information available to allow us to fit higher order coefficients (particularly for some of the more exotic bonds that we might need, such as that between Lead and Germanium, see chapter 6).

We first choose a simple cluster which contains the bond that is being considered; e.g. for the Si-Si bond we chose Si_2H_6. We then calculate the total energy $E(R')$ for the cluster as a function of the Si-Si bond length R', keeping the Si-H bond length fixed, using the quantum chemistry package GAMESS. We then calculate the one-electron part of this energy $E_1(R)$ in the tight-binding formulation. Then we define $U(R)$ by,

$$U(R) = E(R) - E_1(R). \tag{3.15}$$

This method presents two points which have to be dealt with; how does the basis set used by the GAMESS package affect the total energy curve $E(R')$, and the fact that the minimum, R_0', of the total energy curve will in general not be at the

bulk equilibrium bond length d_0. The first point can be tested by comparing the results produced by different basis sets, the second is dealt with by shifting the total energy curve such that the minimum occurs at the required position (when this is known).

To calculate the various U_n's we proceed as follows:

We shift the total energy curve $E(R')$ such that

$$R = R' + (d_0 - R'_0) \tag{3.16}$$

(R'_0 being the point where $E(R')$ is minimised), we then perform a least squares fit of $E(R)$ by

$$E(R) = \sum_{n=0}^{N} E_n \left(\frac{R - d_0}{d_0} \right)^n \tag{3.17}$$

(N is normally about seven for 21 data points).

Next a least squares fit is performed on the one-electron curve $E_1(R)$

$$E_1(R) = \sum_{n=0}^{N} E_{1n} \left(\frac{R - d_0}{d_0} \right)^n . \tag{3.18}$$

(N takes the same value in both equations 3.17 and 3.18). Then from equation 3.15

$$U(R) = \sum_{n=0}^{N} U_n \left(\frac{R - d_0}{d_0} \right)^n = \sum_{n=0}^{N} (E_n - E_{1n}) \left(\frac{R - d_0}{d_0} \right)^n , \tag{3.19}$$

hence equating coefficients,

$$U_n = E_n - E_{1n}. \tag{3.20}$$

This procedure is carried out for each type of bond that was required, in appendix B are the coefficients (with their range of applicability) for all of the bonds that we have worked with.

Source	Basis Set	δZ_1	δZ_2
GAMESS	SV 3-21G	0.26	-0.34
	STO 3G	0.17	-0.25
	STO 6G	0.17	-0.25
Huzinaga	333/33	0.23	-0.33
	533/53	0.24	-0.34
Chadi's Model		0.31	-0.44

Table 3.1: Variations of the Si(111)(2x1) Surface for Different Basis Sets.

To examine the variations caused by using different basis sets, we looked at three provided within the GAMESS package and two published by Huzinaga (1984). When the procedure outlined above is carried out you get a set of curves for $U(R)$ (and also the associated coefficients U_n). While these curves are very similar, they do have obvious differences. What we do not have is a simple method to compare their merit. The best way to examine the effects caused by the basis sets was to examine what they predicted for a particular surface.

The surface that we examined was the Si(111)(2x1), with a Si_7H_{14} cluster (for the details of this surface/cluster see chapter 4). The important details of the surface are that within each unit cell there are two surface atoms (each with three bonds to second layer atoms) which are allowed to be displaced from a bulk terminated position in a direction normal to the surface.

In table 3.1 the predicted displacements for the surface atoms are given, also given are the values published by Chadi (1978). As is clearly obvious from the

results, there are systematic variations from one type of basis set to another. We decided to proceed using the basis sets published by Huzinaga (1984) for two reasons; the Huzinaga basis sets gave the results that were the closest to Chadi's result, and they are available for a very wide range of elements.

Chapter 4

Cluster Construction.

"There is something fascinating about science. One gets such wholesale returns of conjecture out of such a trifling investment of fact."
— Mark Twain, Life on the Mississippi.

4.1 Introduction.

"If the chemist's view of bonding as a local phenomenon is correct, then the understanding of adsorbate-surface bonding should be tractable to the cluster model approach" (Messner, 1979). The experience of quantum chemists is that this is a valid assumption for covalently bonded crystals, therefore we will aim to develop clusters to be used within the tight-binding model.

We are in need of a systematic method to construct the clusters that will be needed to represent an infinite surface. A review of the literature shows that in general quantum chemists work only with 'minimal clusters', i.e. those which represent only one surface cell (Barone, 1987; Nishida, 1978; Redondo, 1977). Those

that do work with larger clusters appear not to have a systematic method of selecting their clusters (Swarts, 1981). The aim of the work presented in this chapter is to set out such a systematic method of cluster construction and enlargement. There are a number of things that any scheme should aim to achieve or take into account;

- Correct local bonding of displaced atoms,
- Surface stoichiometry,
- Pseudo-surfaces,
- Cluster enlargement and convergence of results with increasing cluster size.

The rest of this chapter will be split into the following sections; a consideration of the construction of minimal clusters, the treatment of pseudo-surfaces, cluster enlargement and convergence.

4.2 Construction of Minimal Clusters.

To consider the construction of a minimal cluster, let us start with the following assumptions; that all the atoms are in their bulk terminated positions (i.e. there is no reconstruction or relaxation) with bulk like bonding, and a minimal cluster represents a single surface unit cell. We are now in a position to use some details of the surface under consideration, in particular which crystal face and the expected reconstruction pattern, e.g. the Silicon(111) surface with a (2x1) reconstruction pattern. As a first approximation let us identify only those atoms within a unit cell

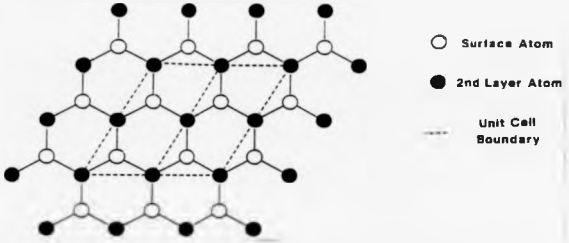

Figure 4.1: The Si(111)(2x1) surface assuming a bulk terminated crystal.

which might be expected to undergo large displacements from their bulk terminated position. In the case of the Si(111)(2x1) surface (see figure 4.1), one might expect only the two surface atoms to be displaced perpendicular to the surface. Since this is a minimal cluster, we will necessarily have the correct stoichiometry. To obtain the correct local bonding, one needs to add additional atoms in their bulk positions, which will remain fixed throughout the calculations. In figure 4.2 are shown the minimal clusters for the three surfaces that will be used to test the method, namely, Si(111)(2x1), Si(100)(2x1) and GaAs(110)(1x1).

4.3 Pseudo-Surfaces.

When we use a cluster to represent the electronic structure of an infinite or semi-infinite system, we necessarily introduce unwanted effects due to the "pseudo-surface" associated with the boundary of the cluster. Since the whole basis of using clusters to model the electronic structure of a crystal depends on the ideal that bonding is a local effect, it is essential that any edge effects are small. However

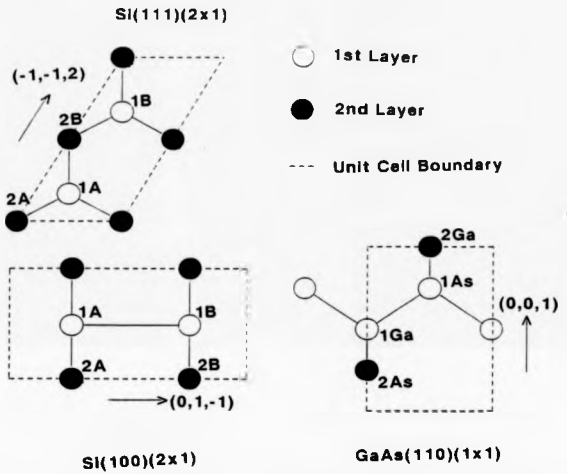

Figure 4.2: Minimal clusters for the Si(111)(2x1), Si(100)(2x1) and GaAs(110)-(1x1) surfaces.

this is not to say that they can be ignored. There are three paths available to deal with the pseudo-surfaces of the cluster;

- do nothing,
- add mono-valent atoms to the boundary of the cluster,
- modify the basis set associated with pseudo-surface atoms.

The first of these approaches is obviously unsatisfactory, but it is the only reasonable option when dealing with extended or poorly defined bonds, i.e. metallic or ionic bonds.

The addition of mono-valent atoms to the surface of a cluster to saturate any dangling hybrids has been used both for calculations in the bulk (Watkins, 1974) and on surfaces (Batra, 1975, 1976a; Swarts, 1981), it is particularly favoured by quantum chemists (Swarts, 1981; Barone, 1986) using ab initio molecular calculations. In covalent crystals the bonds formed are in well defined directions, by correctly positioning the mono-valent atoms the direction of the bonds formed will be the same as those in the crystal. The most commonly used mono-valent atom is hydrogen, it is placed at a distance (which can be found from experiment or calculation) equal to the appropriate bond length. This procedure allows the correct hybridization of the pseudo-surface atoms and stops the artificial dangling hybrids from interacting with the surface under consideration.

The third option of modifying the basis set is less easy to use in general, however for calculations involving a tight-binding SP^3 basis set it is particularly easy to do (Nishida, 1981). For each hybrid on an atom there is exactly one basis function associated with it, given that we can easily identify those dangling hybrids on the

pseudo-surface, we need only exclude the associated basis functions from the basis set.

The various techniques have both positive and negative attributes. Modifying the basis set has the distinct advantage of reducing drastically the size of the basis set. In the case of the Si(111)(2x1) minimal surface cluster considered below the Si_7H_{14} cluster has 42 basis functions, the equivalent Si_7 cluster has only 14 basis functions. The obvious savings in computation have to be weighed against the importance of rehybridization on the small clusters used.

It has been argued that the bonds formed by the addition of hydrogen atoms to the dangling hybrids are so unlike the bonds they replace as to invalidate the results (Appelbaum, 1976). This claim was refuted by Batra and Ciraci (1976b) when they showed that the results that they obtained for Si-H clusters for the Si(111) surface using a self-consistent-field Xα scattered wave model were in good agreement with finite-slab calculations by several other researchers.

In tables 4.1 - 4.3 I have made a comparison of numerical results for a variety of different systems using the two approaches to treating the dangling hybrids. Obviously the errors will be greatest for the smallest clusters, so using the minimal clusters described in figure 4.2 for the Si(111)(2x1), Si(100)(2x1) and GaAs(110)(1x1) surfaces with additional hydrogen atoms or with a reduced basis set, I compared the predicted reconstruction with that calculated by Chadi (1978, 1979). As a measure of the accuracy of the results we used the root of the sum of the squares of the differences between the atom displacements as predicted by us and Chadi.

In all three cases the addition of the hydrogen atoms is preferable to the modification of the basis set. For larger clusters the differences between the two ap-

	δz_1	δz_2	$(\sum \delta^2)^{\frac{1}{2}}$
Chadi	0.31	-0.44	—
Si_7H_{14}	0.25	-0.35	0.11
Si_7	0.25	-0.24	0.21

Table 6.1: Comparison of different treatments of the pseudo-surfaces of a minimal cluster with Chadi's results for the Si(111)(2x1) surface. 'δz' is in the (1,1,1) direction.

	δz_1	δx_1	δz_2	δx_2	$(\sum \delta^2)^{\frac{1}{2}}$
Chadi	0.04	0.46	-0.44	-1.08	—
Si_6H_{12}	0.08	0.44	-0.44	-0.99	0.10
Si_6	0.13	0.42	-0.27	-0.93	0.25

Table 6.2: Comparison of different treatments of the pseudo-surfaces of a minimal cluster with Chadi's results for the Si(100)(2x1) surface. 'δz' is in the (1,0,0) direction and 'δx' is in the (0,1,$\bar{1}$) direction.

	δz_A	δx_A	δz_G	δx_G	$(\sum \delta^2)^{\frac{1}{2}}$
Chadi	0.19	0.19	-0.46	0.35	—
$Ga_3As_3H_{12}$	0.18	0.18	-0.32	0.28	0.14
Ga_3As_3	0.21	0.12	-0.26	0.22	0.25

Table 4.3: Comparison of different treatments of the pseudo-surfaces of a minimal cluster with Chadi's results for the GaAs(110)(1x1) surface. 'δz' is in the (1,1,0) direction and 'δx' is in the (0,0,1) direction.

proaches rapidly disappear.

We have now determined a method to construct minimal clusters and decided what we should do with the pseudo-surfaces. However, it is probably incorrect to assume that a minimal cluster will give acceptable results. We therefore need to be able to systematically enlarge the cluster, and then check that the results for these larger clusters converge towards the expected values for the infinite surface.

4.4 Cluster Enlargement.

To show how we have constructed larger clusters we will consider in detail the Si(111)(2x1) surface. Starting from the minimal cluster shown in figure 4.2, we first let all the atoms in the cluster become moving atoms and then to obtain the correct local bonding for all the moving atoms we have to add new fixed atoms. The cluster so formed is shown in figure 4.3. However this cluster does not display the correct stoichiometry, i.e. the seven moving atoms do not form an integral number of unit cells. We therefore need to add additional fixed and moving atoms

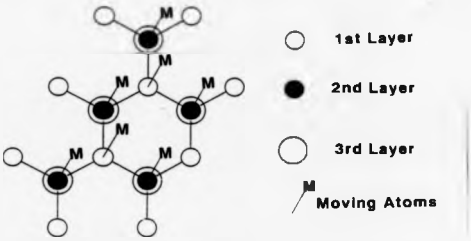

Figure 4.3: Intermediate cluster for the Si(111)(2x1) surface.

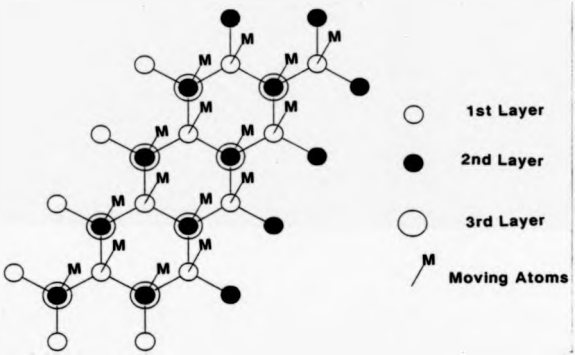

Figure 4.4: Enlarged cluster for the Si(111)(2x1) surface.

to ensure that we obtain the correct stoichiometry and local bonding, giving the cluster shown in figure 4.4. This process can clearly be repeated to give larger clusters which in the limit would reproduce the infinite surface.

We are now in a position to consider how rapidly our results converge with cluster size, as the need for large clusters would undermine the value of the model.

Atom	Si_7H_{14}	$Si_{35}H_{60}$	Chadi
1A(111)	0.24	0.30	0.31
($\bar{1}\bar{1}$2)	-	0.04	0.06
1B(111)	-0.33	-0.39	-0.44
($\bar{1}\bar{1}$2)	-	0.09	0.0
2A($\bar{1}\bar{1}$2)	-	-0.04	-0.13
2B($\bar{1}\bar{1}$2)	-	0.17	0.09

Table 4.4: Atomic displacements in angstroms for the Si(111)(2x1) surface.

Atom	Si_6H_{12}	$Si_{18}H_{28}$	Chadi
1A(100)	0.08	0.11	0.04
(01$\bar{1}$)	0.44	0.44	0.46
1B(100)	-0.44	-0.43	-0.44
(01$\bar{1}$)	-0.99	-1.01	-1.08
2A(100)	-	0.03	0.02
(01$\bar{1}$)	-	0.03	0.12
2B(100)	-	0.00	0.02
(01$\bar{1}$)	-	-0.03	-0.12

Table 4.5: Atomic displacements in angstroms for the Si(100)(2x1) surface.

We also need to establish the accuracy of our results by comparing them with other more accurate calculations. In tables 4.4 to 4.6 we compare our results for the Si(111)(2x1), Si(100)(2x1) and GaAs(110)(1x1) with those of Chadi (1978, 1979)

Atom	$Ga_3As_3H_{12}$ $\theta = 21.3°$	$Ga_{10}As_{10}H_{28}$ $\theta = 25.3°$	Chadi $\theta = 27.4°$	Swarts $\theta = 26.8°$
1As(110)	0.18	0.20	0.19	0.22
(001)	0.16	0.16	0.19	0.37
1Ga(110)	-0.32	-0.40	-0.46	-0.44
(001)	0.28	0.30	0.35	0.48
2Ga(110)	-	0.05	0.07	-
2As(110)	-	0.00	-0.06	-

Table 4.6: Atomic displacements in angstroms for the GaAs(110)(1x1) surface. The angle θ is the tilt of the planes containing the surface atoms relative to the bulk.

and for the GaAs(110)(1x1) also with Swarts et al. (1981) (the atoms mentioned are identified in figure 4.2). The angle θ for the GaAs(110)(1x1) surface is the angle of tilt of the plane containing the surface atoms compared to the bulk. A comparison with Chadi is particularly appropriate since our calculations are similar to his, except we treat the cluster and he treats the infinite surface.

It is clear that the minimal clusters give results that are so similar to the next largest cluster, that in most cases we may restrict our attention to only the minimal cluster. Furthermore, the results for the atom displacements agree very closely with those of Chadi. The differences are of little significance if one considers the approximate nature of the theories.

Chapter 5

Charge Self-Consistency.

"If anybody says he can think about quantum problems without getting giddy, that shows he has not understood the first thing about them."

— Niels Bohr.

5.1 Introduction.

The model as proposed so far, allows a large number of structures to be examined with modest demands on computer resources. The results obtained give good agreement with other tight-binding calculations (Chadi, 1978, 1979, 1983) and calculations by more sophisticated methods (Swarts, 1981).

However it has become clear that tight-binding models can produce results that are misleading. Pandey (1982) working within the 'Density Functional Formalism' in the 'Local Density Approximation' and solving the Kohn-Sham equations self-consistently, made a careful study of the Si(111)(2x1) surface. He demonstrated that the buckling model that we found in the previous chapter was unstable, in

particular he showed that the energy increased monotonically with the degree of buckling. To explain this result he argued as follows: buckling involves a transfer of charge from the atom moving towards the bulk to the atom moving away from the bulk. Such a charge transfer would result in an increase in the intra-atomic Coulomb energy, which would prevent buckling for homopolar semiconductors. A similar argument for the Si(100)(2x1) surface supports the idea of symmetric dimers as proposed by Tromp et al. (1985). However Pandey pointed out that for a surface like that of GaAs(110)(1x1) the buckling predicted by the tight-binding models was likely to happen, since the charge transfer that would be expected to occur would tend to produce neutral atoms on the surface, rather than ions, which would reduce the intra-atomic Coulomb energy.

There is therefore a need to correct our model, so as to take account of charge transfer between atoms. We have considered two methods of achieving this, the first due to Harrison (1984, 1985) involves modifying the term values within the tight-binding formalism, the second is an ad hoc method used by Tománek and Schlüter (1986) in which an additional energy term is included which discriminates against geometries with large charge transfers.

5.2 Harrison's Charge Self-Consistency.

In his paper Harrison (1985) sets out to include some of the effects of charge transfer into his previously published tight-binding model (Harrison, 1980). There are two particular terms that he retains, the first corresponds to an intra-atomic Coulomb repulsion, the second term is an inter-atomic Coulomb repulsion.

Let us consider first the intra-atomic term. If a solid is composed of neutral atoms then the intra-atomic electron energies are given by the term values. However if there is an additional electron on an atom then one would see a shift, W_{nj}, in the eigenvalues ('n' labels the atom and 'j' labels the atomic orbital on the atom). W_{nj} is the change in the energy eigenvalue for one electron when a second is added, and according to Harrison (1985) this corresponds to the "difference between the 1st and 2nd ionization potentials". To a reasonable approximation W_{nj} is the same for both $|S>$ and $|P>$ states on an atom, and hence can be written as W_n. In his paper Harrison tabulates W_n for all the non-transition elements. If the additional charge on an atom is δQ_n then assuming a linear relationship, the change in the energy eigenvalues is $W_n \delta Q_n$.

The inter-atomic Coulomb repulsion, is the change of the energy eigenvalues on one atom due to the presence of an electron on another atom. Assuming that the charges are spherically symmetric and non-overlapping, then the change depends on the inter-atomic distance d_{nm} and the charge on the second atom δQ_m, and is given by $\delta Q_m e^2/d_{nm}$.

The total change in the term value $\Delta\epsilon_n$ of atom n is thus given by,

$$\Delta\epsilon_n = W_n \delta Q_n + e^2 \sum_{m \neq n} \frac{\delta Q_m}{d_{mn}}, \tag{5.1}$$

δQ_n is defined as the difference between the actual number of electrons found on an atom and the number of valence electrons on the neutral atom,

$$\delta Q_n = Q_A(n) - Q_V(n). \tag{5.2}$$

The charge $Q_A(n)$ is the sum of charges associated with the hybrids centred on atom 'n' (Pantelides and Harrison, 1976). Thus if $a_{nk}(J)$ is the eigenvector

component corresponding to hybrid k on atom n for the eigenvalue J, then

$$Q_A(n) = \sum_J \sum_k |a_{nk}(J)|^2, \tag{5.3}$$

the sum J is over occupied states.

It is quite straight forward to evaluate $\Delta\epsilon_n$ (for a given charge distribution) when we restrict our attention to the clusters described earlier. However, when we are looking at the behaviour of an infinite surface it is necessary to consider the infinite set of repeating surface cells, not just the one represented by the cluster, because of the long range of the Coulomb potential. To do this requires the calculation of an infinite lattice sum for the second term in equation 5.1. It is not enough just to calculate $\Delta\epsilon_n$, we need to use them to recalculate the charge distribution and then to iterate the procedure to charge self-consistency.

5.2.1 Infinite Lattice Sum.

Consider the sum in equation 5.1 where it has been extended to cover the infinite plane of repeating unit cells,

$$S = \sum_{m \neq n} \frac{\delta Q_m}{d_{mn}} = \sum_{m \neq n} \frac{\delta Q_m}{|R_n - R_m|}. \tag{5.4}$$

Since we are considering a finite set of charges which are repeated throughout an infinite lattice, the above sum can be written as a finite series of infinite lattice sums

$$S = \delta Q_1 \sum_l \frac{1}{|\rho_1 + r_1 - r_l|} + \delta Q_2 \sum_l \frac{1}{|\rho_2 + r_2 - r_l|} + \cdots - S(n = m), \tag{5.5}$$

r_l is a 2D lattice vector, r_m and ρ_m are vectors in the lattice plane and perpendicular to it, which join atom 'n' to atom 'm' in the cluster (see figure 5.1). The

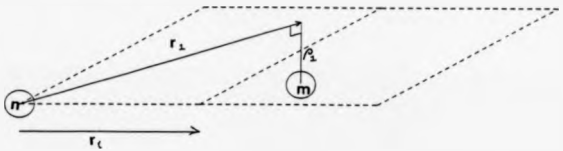

Figure 5.1: Relationship of the vectors used in equation 5.5.

term $-S(n=m)$ signifies that we have to subtract the potential due to an atom interacting with itself, since this is excluded in equation 5.1.

Let us now consider each of the infinite lattice sums, we will Ewalds method (the version used here follows that laid out by Ziman (1963)). Consider the integral

$$\int_0^\infty \exp(-x^2)dx = \frac{1}{2}\sqrt{\pi}, \tag{5.6}$$

since $x \in [0,\infty)$ we can make the substitution $x \to x|z|$, $dx \to |z|dx$, then we have

$$\frac{2}{\sqrt{\pi}}\int_0^\infty \exp(-x^2|z|^2)dx = \frac{1}{|z|}. \tag{5.7}$$

Comparing this to the first term in the above sum, equation 5.5, we find

$$\begin{aligned} S_1 &= \frac{2}{\sqrt{\pi}}\sum_l \int_0^\infty \exp(-x^2|\rho_1 + r_1 - r_l|^2)dx \\ &= \frac{2}{\sqrt{\pi}}\int_0^\infty \exp(-x^2|\rho_1|^2)\sum_l \exp(-x^2|r_1 - r_l|^2)dx. \end{aligned} \tag{5.8}$$

The problem with both the original form of the sum S_1 and that given in equation 5.8 is that they both diverge for large 'l'. Since in the end we need to sum the effect of both positive and negative lattice sums, the divergences at infinity will cancel out because of the overall charge neutrality of the system. We therefore need to find a form of the above equation which will converge quickly and allow

us to identify and hence exclude the terms at infinity which cause the divergence, we also need to exclude the term corresponding to $|r_m + \rho_m - r_l| = 0$.

Consider the function $F(r,\rho)$ which has the periodicity of the lattice,

$$F(r,\rho) = \frac{2}{\sqrt{\pi}} \sum_l \exp(-\rho^2 |l - r|^2). \tag{5.9}$$

It can therefore be written as a Fourier Series

$$F(r,\rho) = \sum_g F_g \exp(-ig.r), \tag{5.10}$$

where

$$F_g = \frac{1}{A} \int \frac{2}{\sqrt{\pi}} \sum_l \exp(-|l - r|^2 \rho^2) \exp(-ig.r) dr, \tag{5.11}$$

the integral being over the whole 2D lattice of total area 'A'. Introducing a factor $\exp(ig.l) = 1$ and then observing that each term in the summation is equivalent,

$$F_g = \frac{N}{A} \frac{2}{\sqrt{\pi}} \int \exp(-r^2 \rho^2 - ig.r) dr, \tag{5.12}$$

N being the total number of lattice cells. This integral can be evaluated to give

$$F_g = \frac{2\sqrt{\pi}}{\Delta_2} \frac{1}{\rho^2} \exp(-g^2/4\rho^2), \tag{5.13}$$

Δ_2 being the area of a single lattice cell, hence

$$\frac{2}{\sqrt{\pi}} \sum_l \exp(-|l - r|^2 \rho^2) = \frac{2\sqrt{\pi}}{\Delta_2} \sum_g \frac{1}{\rho^2} \exp(-g^2/4\rho^2) \exp(ig.r). \tag{5.14}$$

Taking the second form for S_1 in equation 5.8, and splitting the integral at some point G and substituting from above for the first integrand and a change of variables in the second gives

$$\begin{aligned} S_1 &= \frac{2\sqrt{\pi}}{\Delta_2} \sum_g \exp(ig.r) \int_0^G \frac{1}{x^2} \exp(-x^2 |\rho|^2) \exp(-|g|^2/4x^2) dx \\ &+ \sum_l \frac{1}{|\rho_l + r_l - r_l|} \operatorname{erfc}(G|\rho_l + r_l - r_l|) \end{aligned} \tag{5.15}$$

(erfc(x) being the complimentary error function). If we now expand the term $\exp(-x^2|\rho|^2)$, we obtain for the first term in equation 5.15,

$$S_{1,1} = \frac{2\sqrt{\pi}}{\Delta_2} \sum_g \exp(ig.r) \int_0^G \sum_{n=0} \frac{1}{n!} (-x^2|\rho|^2)^n \frac{1}{x^2} \exp(-|g|^2/4x^2) dx, \qquad (5.16)$$

following a change in variables, and using the incomplete gamma function $\Gamma(m, x)$, this becomes

$$S_{1,1} = \frac{2\sqrt{\pi}}{\Delta_2} \sum_g \frac{\exp(ig.r)}{|g|} \sum_{n=0} \frac{1}{n!} \left(\frac{-|\rho|^2|g|^2}{4} \right)^n \Gamma(-(n-1/2), |g|^2/4G^2). \qquad (5.17)$$

If each plane of atoms in the sum was neutral then the singularities at $|g| = 0$ cancel. We are however dealing with a slightly different problem in which we have only overall neutrality of the surface charge layer unit cell. Therefore we must consider the $|g| = 0$ terms more carefully to ensure that only 'equal' infinities are cancelled. Using the reduction formula for the incomplete gamma function

$$\Gamma(\nu + 1, x) = \nu\Gamma(\nu, x) + x^\nu e^{-x}, \qquad (5.18)$$

one can show that

$$\begin{aligned} \Gamma(-n + 1/2, x) &= \frac{1}{\sqrt{\pi}} \Gamma(-n + 1/2)\Gamma(1/2, x) \\ &- \sum_{p=0}^{n-1} \frac{\Gamma(-n + 1/2)}{\Gamma(-n + 3/2 + p)} x^{(-n+p+1/2)} \exp(-x). \end{aligned} \qquad (5.19)$$

Picking out terms for $|g| = 0$ in equation 5.17 and using the following limits;

$$\begin{aligned} \lim_{g \to 0} e^{ig.r} &= 1, \\ \lim_{g \to 0} e^{-|g|^2/4G^2} &= 1, \\ \lim_{g \to 0} \Gamma(1/2, |g|^2/4G^2) &= \sqrt{\pi}, \end{aligned} \qquad (5.20)$$

we obtain

$$\frac{2\sqrt{\pi}}{\Delta_2|g|} \sum_{n=0} \frac{1}{n!} \left(\frac{-|\rho|^2|g|^2}{4} \right)^n \left[\Gamma(-n + 1/2) - \frac{|g|}{2G} \sum_{p=0}^{n-1} \frac{\Gamma(-n + 1/2)}{\Gamma(-n + 3/2 + p)} \left(\frac{4G^2}{|g|^2} \right)^{n-p} \right]. \qquad (5.21)$$

If we now pick out terms in different orders of $|g|$ we get,

$$\frac{2\pi}{\Delta_2|g|} + \frac{2\sqrt{\pi}}{\Delta_2 G}\sum_{n=0}\frac{(-|\rho|^2G^2)^n}{n!(2n-1)} + \mathrm{O}(|g|), \tag{5.22}$$

which can be expressed as

$$\frac{2\pi}{\Delta_2|g|} - \frac{2\sqrt{\pi}}{\Delta_2 G} + \frac{2\sqrt{\pi}}{\Delta_2}\int_{1/G}^{\infty}(\exp(-|\rho|^2/u^2) - 1)du + \mathrm{O}(|g|). \tag{5.23}$$

If the sum in equation 5.5 is now carried out, we obtain

$$S = \frac{2\pi}{\Delta_2|g|}\sum_s \delta Q_s + \text{ terms in}|\rho| \text{ and} G, \tag{5.24}$$

this leading term must have value zero (due to the overall neutrality of the unit cell), hence the $|g| = 0$ term in $S_{1,1}$ needs to be replaced by

$$-\frac{2\sqrt{\pi}}{\Delta_2 G} + \frac{2\sqrt{\pi}}{\Delta_2}\int_{1/G}^{\infty}(\exp(-|\rho|^2/u^2) - 1)du. \tag{5.25}$$

The last term in equation 5.5 is accounted for by excluding the appropriate term in equation 5.15 for the case when $|\rho_i + r_i - r_l| = 0$.

An important condition that we use in the above analysis is that each unit cell has charge neutrality, in the case of the clusters that we use in our calculations, it does not automatically follow that the atoms that form a unit cell will be charge neutral, because of the transfer of charge to the Hydrogen atoms in the cluster. So we apply a small correction factor α that produces charge neutrality within the unit cell, α being defined by

$$\alpha\sum_n Q_A(n) = \sum_n Q_V(n). \tag{5.26}$$

So the adjusted charges $Q'_A(n)$ are given by

$$Q'_A(n) = \alpha Q_A(n). \tag{5.27}$$

5.2.2 Iterative Processes for Solving the Charge Self-Consistent Problem.

The idea of charge self-consistency is that if one has a set of charges on atoms $Q_A(n)$, which have an associated set of $\Delta\epsilon_n$'s, then the charges produced on the cluster are those that we started with, i.e.

$$\underline{Q}_A = \underline{f}(\underline{\epsilon}_n + \Delta\underline{\epsilon}_n(\underline{Q}_A)), \tag{5.28}$$

where this represents a highly non-linear system of simultaneous equations. We have used two schemes to solve this problem, one is an iterative procedure due to Anderson (Anderson, 1965; Dederichs, 1983), the second is a least-squares minimization method. The advantage of the first is that it is generally quick, the second is much more robust and is likely to work even in situations when the iterative method is going to fail .

Anderson's Method.

In Anderson's method we have a series of inputs into a non-linear system $\underline{\rho}_n$, which produce a set of outputs $\underline{\sigma}_n$,

$$\underline{\sigma}_n = \underline{f}(\underline{\rho}_n). \tag{5.29}$$

Two successive inputs $\underline{\rho}_n$ and $\underline{\rho}_{n-1}$ define a hyper-line through the variable space under consideration. Two successive outputs $\underline{\sigma}_n$ and $\underline{\sigma}_{n-1}$ define a second hyper-line through the same variable space. These lines are given by,

$$\bar{\underline{\rho}}_n = \alpha_n\underline{\rho}_n + (1-\alpha_n)\underline{\rho}_{n-1}, \tag{5.30}$$

$$\bar{\underline{\sigma}}_n = \alpha_n\underline{\sigma}_n + (1-\alpha_n)\underline{\sigma}_{n-1}. \tag{5.31}$$

Now in general these two hyper-lines do not intersect. What we do is to find the optimum value of α_n such that $(\underline{\hat{\rho}}_n - \underline{\tilde{\rho}}_n)^2$ is minimized, i.e.

$$\frac{d}{d\alpha_n}(\underline{\hat{\rho}}_n - \underline{\tilde{\rho}}_n)^2 = 0, \tag{5.32}$$

defining $r_n = \underline{\rho}_n - \underline{\varrho}_n$

$$\alpha_n = \frac{r_{n-1} \cdot (r_{n-1} - r_n)}{(r_{n-1} - r_n)^2}. \tag{5.33}$$

Then to evaluate the input for the next iteration $\underline{\rho}_{n+1}$, one introduces a mixing factor α'

$$\underline{\rho}_{n+1} = \alpha' \underline{\tilde{\varrho}}_n + (1 - \alpha') \underline{\hat{\rho}}_n \tag{5.34}$$

$$\alpha' \in (0, 1], \tag{5.35}$$

the actual value of α' must be determined empirically.

This method can be readily generalized to hyper-planes, consider

$$\underline{\hat{\rho}} = (1 - \sum_{i=1} \alpha_i) \underline{\rho}_N + \sum_{i=1} \alpha_i \underline{\rho}_{N-i}, \tag{5.36}$$

$$\underline{\tilde{\varrho}} = (1 - \sum_{i=1} \alpha_i) \underline{\varrho}_N + \sum_{i=1} \alpha_i \underline{\varrho}_{N-i}. \tag{5.37}$$

If we define

$$E_m = \underline{\varrho}_m - \underline{\rho}_m, \tag{5.38}$$

$$D_m = E_N - E_{N-m}, \tag{5.39}$$

$$\bar{E} = \underline{\tilde{\varrho}} - \underline{\hat{\rho}}, \tag{5.40}$$

$$\bar{E}^2 = (E_N - \sum_{i=1} \alpha_i D_i)^2. \tag{5.41}$$

Let D be a matrix with rows D_j and let α be a column vector with terms α_i, then

$$DD^T \alpha = DE_N^T, \tag{5.42}$$

$$\alpha = (DD^T)^{-1} DE_N^T. \tag{5.43}$$

The advantage of using the hyper-planes is that more of the variable space is covered using information from a greater number of previous iterations. The problems are that the calculations are longer and difficulties due to linear dependence arise.

While the above method is generally quick, it can however fail for the more pathological forms of equation 5.28. For these situations we use a different method which does not depend so much on the information in the vectors $\underline{\rho}_n$ and $\underline{\varrho}_n$.

Least Squares Minimisation Method.

We define a single valued function

$$L(\underline{\rho}_N) = (\underline{\varrho}_N - \underline{\rho}_N)^2. \tag{5.44}$$

We then minimise the function L with respect to the vector $\underline{\rho}_N$. This particular form of optimization is known as a least-squares problem. There are many algorithms in the literature which deal with this type of problem. For computational ease we used an algorithm published by Gill and Murray (1978) and implemented by NAG. The advantage of this method is that it is unaffected by many of the convergence problems associated with iterative procedures.

5.3 Charge Discrimination Model.

While the previous method of obtaining a charge self-consistent solution works as it is supposed to, it does suffer from a single major drawback. That is the large increase in the time required to find a solution. This stems from the fact that

at each geometry of the cluster it is necessary to calculate the one-electron terms some 30-60 times, compared with once for the non-self-consistent case. What would be useful is an ad hoc method which achieves much the same effect as the self-consistent method but requires much less computation, preferably a single calculation at each geometry.

The prime requirement that comes out of Pandey's (1982) analysis is that one should try to produce neutral atoms on the surface. One way of doing this was used by Tománek and Schlüter (1986), in which they introduce a 'penalty function' which discriminated against charge transfer. The total energy equation becomes

$$E_T = \sum_i \epsilon_i + \sum_{\text{bonds}} \sum_n U_n \epsilon^n + V \sum_{\text{atoms}} (Q_A(n) - Q_V(n))^2, \qquad (5.45)$$

where V is a parameter which Tománek and Schlüter chose to be $V = 1$eV.

Below are presented the results for the same surfaces discussed in chapter 4.

5.4 Results for the Charge Self-Consistent and Charge Discrimination Models.

In tables 5.1 to 5.3 are the results for the Si(111)(2x1), Si(100)(2x1) and GaAs(110)-(1x1) surfaces. The displacement directions and atom labels are the same as in tables 4.4 to 4.6, and are identified in figure 4.2. Also given are the charges associated with each atom as evaluated by equations 5.3 and 5.27. The columns are labelled by SC (self-consistent method), NSC (non-self-consistent method) and δQ^2 (charge discrimination method).

For the Si(111)(2x1) structure the introduction of charge self-consistency clearly

Atom	SC	NSC	δQ^2	δQ^2	Pandey
1A(111)	0.02	0.24	0.02	0.29	-0.26
1B(111)	0.02	-0.33	0.02	-0.37	-0.26
Charge 1A	0.00	-0.73	0.00	-0.72	0.00
Charge 1B	0.00	0.73	0.00	0.72	0.00

Table 5.1: Comparison of local minima using the self-consistent (SC), non-self-consistent (NSC) and charge discrimination (δQ^2) models for the Si(111)(2x1) surface. Also given is Pandey's (1982) result.

shows that the bulk terminated surface prefers a (1x1) structure, as proposed by Pandey (1982), rather than the (2x1) structure predicted by the non-self-consistent model. The SC result does not agree with Pandey's prediction for the relaxation that occurs. The charge discrimination model has multiple local minima, one which relates to the self-consistent minimum and one which relates to the non-self-consistent minimum. It would seem that the charge discrimination model is best used as a quick way of estimating the position of self-consistent minima.

For the Si(100)(2x1) surface, one finds that charge self-consistency makes very little difference and a buckled dimer is still predicted. This is despite the large charge transfer involved. Included in table 5.2 is the most stable of the symmetric dimers and the energies of each minimum. The results are clearly in dispute with the predictions of Pandey (1982) and the observations of Tromp et al. (1985), both of which suggest that the surface consists of symmetric dimers.

For the GaAs(110)(1x1) surface, I have been unable to find any stable local

Atom	SC	NSC	δQ^2	SC
1A(100)	0.05	0.08	0.08	-0.19
$(01\bar{1})$	0.49	0.44	0.42	0.75
1B(100)	-0.48	-0.44	-0.46	-0.19
$(01\bar{1})$	-1.01	-0.99	-1.01	-0.75
Charge 1A	-0.40	-0.54	-0.53	0.00
Charge 1B	0.40	0.54	0.53	0.00
Energy	-634.79	-635.18	-634.61	-634.59

Table 5.2: Comparison of local minima using the self-consistent (SC), non-self-consistent (NSC) and charge discrimination (δQ^2) models for the Si(100)(2x1) surface. The final column is the most stable of the symmetric dimers, and the energies are in eV.

Atom	SC	NSC	δQ^2
	—	$\theta = 21.3°$	$\theta = 23.7°$
1As(110)	—	0.18	0.20
(001)	—	0.16	0.16
1Ga(110)	—	-0.32	-0.36
(001)	—	0.28	0.30
Charge 1As	—	-0.50	-0.49
Charge 1Ga	—	0.50	0.49

Table 5.3: Comparison of local minima using the self-consistent (SC), non-self-consistent (NSC) and charge discrimination (δQ^2) models for the GaAs(110)(1x1) surface. The angle θ is the tilt of the planes containing the surface atoms relative to the bulk.

minimum for the self-consistent method[1]. The only minimum found for the charge discrimination model is given in table 5.3 and it is close to that for the non-self-consistent method. If one is to believe the experience gained with the other two surfaces, then one should expect the self-consistent minimum to be in the region of the two minima given in table 5.3.

[1]The self-consistent minimum published for this surface by Dr V.Dwyer, Dr B.W.Holland and myself in the Proceedings of the Second International Conference on the Structure of Surfaces (Springer Series in Surface Science 11, 320, 1988, editors: J.F. van der Veen and M.A. Van Hove) is incorrect.

Chapter 6

Structure of the α-phase of Ge(111)$\sqrt{3}$x$\sqrt{3}$-Pb.

"It is also a good rule not to put too much confidence in experimental results until they have been confirmed by theory."

— Sir Arthur Eddington.

6.1 Introduction.

One of the areas of interest to surface science is the structure of metal/semiconductor interfaces, particularly during the period of formation. Given that there are a large number of metal/semiconductor systems available to study, why should a Lead/Germanium system be of particular interest?

While it is true that the Lead/Germanium system is part of a small family of IV/IV metal/semiconductor systems and is of interest in itself, there are other considerations. It is known that Lead films are superconductive materials impor-

tant in Josephson technology. Another possibility for the system is that given the differences in melting point between the Lead and Germanium, the system represents a possibility for the study of 2D liquids (Ichikawa, 1983). A more practical consideration from the position of the analysis of experimental results, is that "there is negligible alloying of Lead with Germanium, so that interdiffusion of lead atoms into the bulk Germanium lattice sites can be excluded from model structures" (Li and Tonner, 1988).

This chapter will continue with a review of published work for this system, followed by the work done using the tight binding model, finishing with a comparison of the results with experiment.

6.2 Review of Published Work.

It has been established over several years by a number of authors (Ichikawa, 1983; Li and Tonner, 1988; Le Lay and Métois, 1983, 1984; Feidenhans'l et al, 1986) that two distinct structures exist for low coverages of Lead on a Germanium(111) surface. Both have a $\sqrt{3}x\sqrt{3}R30°$ reconstruction, the distinguishing factor being the number of Lead atoms per unit surface cell. For the structure with lowest density (known as the α-phase) all the previously named authors agree that there is one Lead atom per unit cell. The more dense structure (β-phase) is still a point of debate, with some authors claiming that it has three Lead atoms per unit cell (Li and Tonner, 1988; Le Lay and Métois, 1983, 1984), while others claim four Lead atoms per unit cell (Ichikawa, 1983; Feidenhans'l et al, 1986). Depending on the number of Lead atoms per unit cell the various authors propose at least three

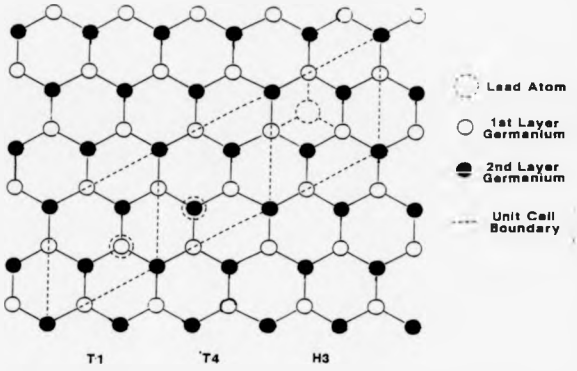

Figure 6.1: The three possible sites for a single Pb atom on a Germanium substrate with $3m$ symmetry.

different structural models for the β-phase.

For the α-phase the principle question that arises is: what is the adsorbate / substrate registry (i.e. where within the unit cell does the Lead atom reside)? If we assume "that the $3m$ symmetry from the bulk crystal is imposed on the $\sqrt{3}$x$\sqrt{3}$R30° unit cell of the surface" (Feidenhans'l et al, 1986), then there exists only three possible models, as shown in figure 6.1. The Lead atom may sit above a first layer Germanium atom (T_1 site), above a Second layer Germanium atom (T_4 site) or above a fourth layer Germanium atom (H_3 site). Most of the papers published on this system have concentrated on the more complex β-phase. Feidenhans'l et al (1986) examined the system using Surface X-ray Diffraction (SXD) and concluded that for the α-phase the T_4 site was the one found occupied on the

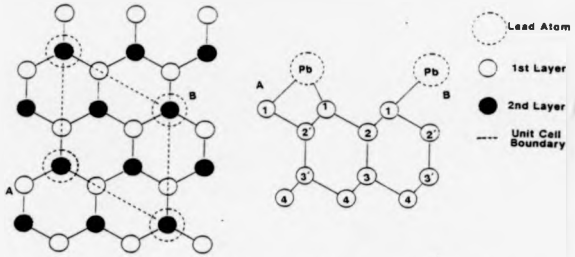

Figure 6.2: The labelling system used by Pedersen (1987, 1988).

surface. This was in agreement with total energy pseudopotential calculations for the Si(111)$\sqrt{3}$x$\sqrt{3}$R30°-Al structure (Northup, 1984) and Si(111)$\sqrt{3}$x$\sqrt{3}$R30°-In structure (Nichols et al, 1985).

In an extension to the analysis of the Surface X-ray Diffraction Pedersen (1987, 1988) was able to estimate the displacements in the top four layers of Germanium from their bulk position, as well as the position of the Lead atom. In figure 6.2 the labelling system used by Pedersen is shown. In his thesis Pedersen (1988) also produced results using Keating's Elastic Strain Model (Keating, 1966). In table 6.1 are the displacements given by Pedersen, it was assumed that the fifth layer was held fixed for the elastic strain model.

6.3 Tight-Binding Calculations.

In figure 6.3 we give the three clusters that we used to compare the three possible adsorption sites (T_1, T_4, H_3). For the three structures we minimised the total

Atom	Direction	Exp.	Keating
Pb	v	0.634	-0.136
1	v	0.567	-0.003
	h	0.156	0.136
2'	v	0.513	-0.307
2	v	0.663	0.133
3'	v	0.513	-0.257
3	v	0.663	0.103
4	h	-0.072	-0.064

Table 6.1: Displacements, in Å, from bulk positions for the Germanium atoms and a starting position for the Lead atom such that the Ge-Pb bond length is 2.84 Å. 'h' indicates in-plane displacements towards the adatom, 'v' indicates displacements normal to the surface (Pedersen, 1988).

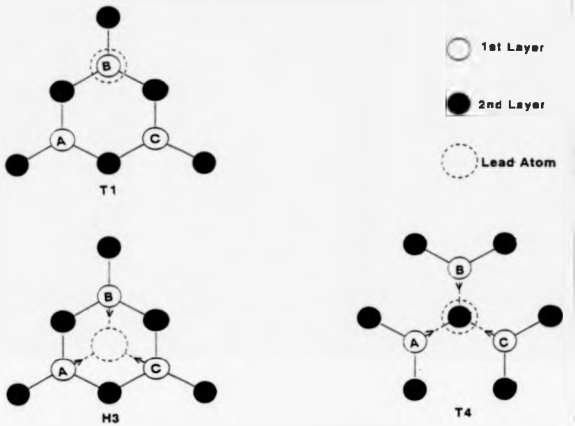

Figure 6.3: The clusters used in the ETBM calculations for each of the three sites T_1, T_4 and H_3. The arrows indicate the positive direction for the in-plane displacements.

energy with respect to the displacements normal to the surface for the Pb and three 1st layer Ge atoms, in the case of the T_4 and H_3 sites the in plane displacements of the surface atoms were also included. In the T_4 and H_3 models all the first layer Ge atoms are equivalent and have the same size displacements. In the T_1 model the three surface atoms are inequivalent and are allowed to vary independently.

To determine the lowest energy structure we proceed as follows. For a given cluster after optimisation we have a total energy E_0. Then if E_B is the energy for the cluster without the Pb atom in the bulk terminated (unrelaxed) state, and E_{Pb} is the energy of an isolated Pb atom, then the energy ΔE_a gained by adsorption of the Pb and relaxation is

$$\Delta E_a = E_0 - E_B - E_{Pb}. \tag{6.1}$$

Since E_{Pb} is common to all three clusters the most stable structure will be that for which

$$\Delta E = E_0 - E_B \tag{6.2}$$

is lowest.

The results obtained are shown in table 6.2, The displacements are relative to a starting structure where the Ge atoms are in the bulk terminated positions and the Pb atom is placed so that the Pb-Ge distance corresponds to the bond length of 2.84Åfound in the quantum chemistry calculation for $PbGeH_6$, which was made using the Gaussian 82 package.

Site	T_1	T_4	H_3
Ge_A	-0.57 - -0.01	-0.49 0.01 -0.02	-0.47 0.00 -0.01
Ge_B	-0.39 - -0.06	ditto	ditto
Ge_C	-0.57 - -0.01	ditto	ditto
Pb	-0.41 - 0.08	-0.35 - 0.05	-0.36 - 0.04
ΔE	-36.03	-55.04	-49.08

Table 6.2: Atomic displacements:-Å, atomic charges:-e and energies:-eV for the three clusters. The first figure in each box is the normal displacement, the second is the displacement along the arrow directions of figure 6.3 in the surface plane and the third figure is the atomic charge.

6.4 Conclusions.

The tight binding calculation of the energy values show that the T_4 site is the stable structure in agreement with the SXD studies (Feidenhans'l et al, 1986). The main features of the structure are a strong contraction of the first layer Ge atoms towards the bulk and a slight increase in the Pb-Ge bond length.

The displacements given by Pedersen for both the experimental values and those produced by Keating's elastic strain model appear to be in poor agreement with each other and the results produced by the tight binding model. This could in part be due to the difference in the number of layers used in the calculations, also the errors in the experimental work are large. Pedersen (1987) quotes the following for the distance between the adatom and the atom labelled 3', 5.04±0.98 Å.

	Bulk	Experimental	Keating	ETBM
Ge_1-h	-	0.156±0.028	0.136	0.01
Pb-Ge_1	1.67	1.72±0.13	1.52	1.81
Pb-Ge_2	2.48	2.44±1.20	2.64	2.13
Pb-$Ge_{2'}$	"	2.59±0.98	2.64	"
Ge_1-Ge_2	0.81	0.72	0.68	0.32
Ge_1-$Ge_{2'}$	"	0.87	1.12	"

Table 6.3: Comparison for the T_4 site of the separations between various layers of the Pb-Ge(111) system. The first column gives the values for bulk like starting position given before (with the Pb-Ge bond length equal to 2.84 Å), experimental errors are given when known, measurements in Å.

A more useful comparison of the three models is given by the separations of the adatom and the top two layers of Germanium atoms. In table 6.3 we give the in-plane displacement of the surface Ge atoms and the normal separations between the adatom and the atoms labelled '1', '2' and '2'.

Due to the rather large uncertainties in the experimental data it is not possible to say whether the tight binding calculation is right or wrong. The only really discernible fact is the difference in the in-plane displacement of the Ge_1 atoms. This may be improved upon if the tight binding calculation is repeated with more layers.

Chapter 7

Reconstruction of the (100) Surface of Cubic Silicon Carbide.

"This shows how much easier it is to be critical than correct."

— Benjamin Disraeli.

7.1 Introduction.

The surfaces of Cubic Silicon Carbide (β-SiC), have only recently come under investigation. This has probably been due to problems associated with growing suitable crystals, these appear to have been overcome with the growth of β-SiC on the (100) surface of Silicon by the Chemical Vapour Deposition (CVD) method (Nishino, 1983).

There are a number of reasons why one might wish to study the surfaces of β-SiC. It is the only IV/IV zincblende compound, and is a 'wide band-gap' semiconductor (hence it can operate at higher temperatures). From the theoretical

point of view it is an interesting stepping stone from the homopolar semiconductors (Si, Ge) to the polar semiconductors (GaAs etc).

At the present time the experimental work available does not give a consistent view of the structures to be found on the various surfaces. To quote from Kaplan (1986):

> "SiC surface composition and structure appear to be sensitive to the method of surface preparation".

In this chapter I shall be concentrating on some results produced by Dayan (1985, 1986) for which there is some independent support (Kaplan, 1986; Takai et al., 1985), the chapter will continue by looking at this work published by Dayan, going on to the ETBM calculations performed and followed by some conclusions.

7.2 Review of M. Dayan's Results (1985, 1986).

In his work Dayan takes his as received samples and anneals them to desorb the surface oxygen. When a sample is treated in this way one of two structures appears, the structures are characterised by the different temperatures of the substrate at which they appear. On further annealling one of the structures undergoes additional transitions until both exhibit the same c(2x2) structure. Results from Auger Electron Spectroscopy (AES) imply that in all of these structures Silicon is to be found in the uppermost layer (Dayan, 1986). If the samples are further heated another transition is observed to a (2x1) structure with Carbon in the surface layer (Dayan, 1985). In figure 7.1 we give the sequence of events as observed by Dayan. The reasons for this behaviour are unclear but may be associated with

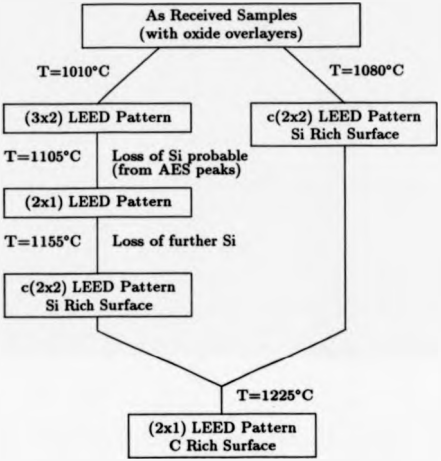

Figure 7.1: The sequence of transitions observed on the SiC(100) surface by Dayan. The temperature 'T' is the transition temperature.

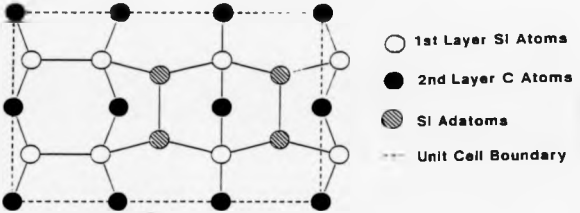

Figure 7.2: Dayan's (1986) proposed model for the Si-(3x2) structure.

the fabrication process.

In his analysis of the results in his papers Dayan makes the following suggestions for the structures observed:

- Both the Carbon rich (2x1) and the Silicon rich c(2x2) structures are in the form of simple dimers of the type found on the Si(100)(2x1) surface.
- For the Si-(3x2) structure, the model shown in figure 7.2 with four Silicon adatoms is proposed.
- The Si-(2x1) structure consists of three Si atoms per unit cell. Two of the Silicon atoms are bonded to Carbon atoms on the second layer and to each other to form a simple dimer. The Silicon adatom then forms a bridge between adjacent dimers along the direction of the dimers as shown in figure 7.3.

For this adatom model one might expect adjacent adatoms to form a dimer and hence a (2x2) structure, which is not observed. Dayan (1986) uses the following argument to explain the lack of dimerisation:

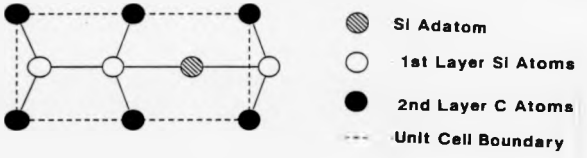

Figure 7.3: Dayan's (1986) proposed model for the Si-(2x1) structure.

"If weak interactions exist along the row direction, one would be puzzled by the lack of dimerisation along that same direction. This may be solved by assuming an electronic configuration which does not allow any interaction between the extra Silicon atoms. This is the configuration without any hybridisation, where the bonding to the Silicon layer is done by the 'P' electrons and the pair of 'S' electrons remain as a lone pair."

In the next section we present the calculations performed on some of the structures identified by Dayan. Simple dimer models are examined for the C-(2x1) and Si-c(2x2). Three possible models are considered for the Si-(2x1) structure, two of them using Silicon adatoms. The two models with adatoms are also compared to their (2x2) structure to see if they are energetically favoured.

7.3 Tight-Binding Calculations.

7.3.1 Structures Examined.

In figure 7.4 we give diagrams of the C-(2x1) and Si-c(2x2) unit cells. Both struc-

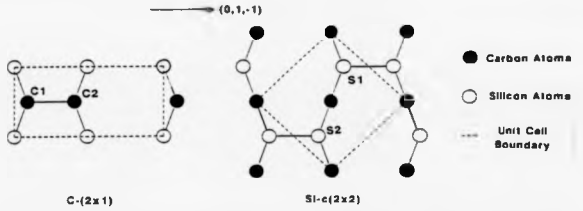

Figure 7.4: Surface unit cells for the C-(2x1) and Si-c(2x2) structures assuming simple dimers.

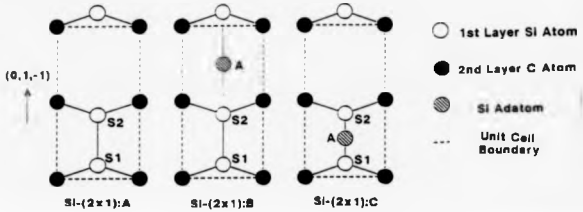

Figure 7.5: Three models for the Si-(2x1) structure.

tures are based on a bulk terminated surface with adjacent surface atoms forming dimers. The (100) direction is normal to the surface plane, the atom labelling and directions indicated are used in section 7.3.3.

In figure 7.5 are the three models that were examined for the Si-(2x1) structure. The first is a simple bulk terminated crystal with adjacent surface atoms forming a dimer, similar to that on the Si(100)(2x1) surface. The second is Dayan's adatom model, with the adatom bridging between adjacent rows of dimers. The final model considered is another adatom model, with the adatom breaking the bond

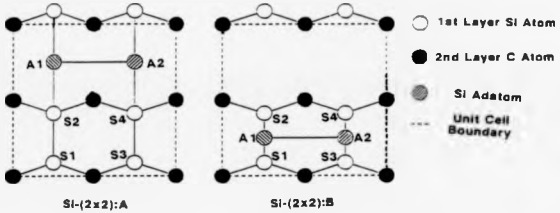

Figure 7.6: The (2x2) structures formed by the adatom models for the Si-(2x1) structure if dimerisation occurs.

forming the dimer in a similar way to that proposed by Barone et al. (1985) for Oxygen on the Si(100)(2x1) surface.

To test Dayan's hypothesis that in an adatom model for the Si-(2x1) structure the adatoms would not form dimers, we also have looked at the (2x2) structure that would be formed if this was the case. The appropriate models are given in figure 7.6.

7.3.2 Comparison of the Energy for Different Clusters.

To test Dayan's hypothesis, it is necessary to compare the total energy of the (2x2) with that of the (2x1) structure to see which of the two is more stable. We proceed as follows:

Consider the structure for Dayan's adatom model in its (2x2) configuration (figure 7.6 model A). We now remove the bond between the two adatoms and require that the left and right sections of the unit cell be similar. Then we obtain two adjacent (2x1) unit cells (c.f. figure 7.5 model B). The only difference between

the two cases is the number of Si-Si bonds, this is also true for the second adatom model. If we now compare the two different (2x2) models we find that they have the same number of atoms of each type and that the only difference is the number of Si-Si bonds. As each of the four possible cases can be represented by the same set of atoms their total energies can easily be compared.

Let us label the total energy defined in previous chapters E_{pq}, $p \in \{ A, B \}$ $q \in \{ 0, 1 \}$, the 'A' and 'B' indicate either the first or second adatom models, the '1' and '0' indicate whether the adatoms are bonded to each other or not.

Normally the total energy is expressed as

$$E_T = \sum_i \epsilon_i + \sum_{\text{bonds}} \left(U_1 \frac{(d - d_0)}{d_0} + U_2 \frac{(d - d_0)^2}{d_0^2} + \cdots \right) \qquad (7.1)$$

neglecting the U_0 terms, if we are to compare different structures we need to retain these terms (see Chadi, 1984). So we have

$$E'_T = E_T + \sum_{\text{bonds}} U_0, \qquad (7.2)$$

splitting this second term into Si-Si bonds and other bonds and then neglecting the sum over other bonds (since they are the same for all four structures) we obtain

$$E''_T = E_T + \sum_{\substack{\text{Si-Si} \\ \text{bonds}}} U_0. \qquad (7.3)$$

Chadi (1984) gives a value of $U_0 = 4.1$ eV for a Si-Si bond.

7.3.3 Results.

In the results that are presented here all the displacements are in angstroms, the directions and atom labelling are as indicated in figures 7.4-7.6. The starting configuration was the bulk terminated crystal, with the adatoms being placed such

Structure	Atom	(1,0,0)	(0,1,-1)	charge
C-(2x1)	C_1	-0.29	0.81	0.00
	C_2	-0.29	-0.81	0.00
Si-c(2x2)	S_1	0.06	0.23	-0.77
	S_2	-0.17	-0.56	0.77

Table 7.1: Dispacements in angstöms for the C-(2x1) and Si-c(2x2) structures, charge in atomic units.

that tetrahedral bonding was maintained with the top layer Silicon atoms and the SiC bond length of 1.88Å was used.

In table 7.1 are the results for the C-(2x1) and Si-c(2x2) models. For the C-(2x1) model a simple symmetric dimer was obtained. For the Si-c(2x2) model a buckled dimer was found to have lowest energy, this despite the very large transfer of charge involved, we were unable to find any stable dimers with lower charge transfer for this model.

In table 7.2 are the results for the Si-(2x1) models, Si-(2x1):A being a symmetric dimer. Both the adatom models display unsymmetric displacements, and rather than compare the energies of the two adatoms models as shown in section 7.3.2 to determine which is the most stable, this will be done as part of the analysis for the (2x2) models.

For the two (2x2) models the clusters were allowed only very symmetric relaxations when trying to optimise the structure (this is because they were needed only as comparison for the (2x1) structures). In particular for Si-(2x2):A the

Structure	Atom	(1,0,0)	(0,1,-1)	charge
Si-(2x1):A	S_1	-0.06	0.37	0.00
	S_2	-0.06	-0.37	0.00
Si-(2x1):B	S_1	0.03	0.13	0.02
	S_2	0.00	-0.30	-0.03
	A	0.51	-0.10	0.01
Si-(2x1):C	S_1	0.08	0.32	0.30
	S_2	-0.25	0.63	-0.21
	A	0.61	0.04	-0.09

Table 7.2: Displacements in angstroms for the three models for the Si-(2x1) structure, charge in atomic units.

atoms labelled 'S_i' have the same normal displacements and equal in-plane displacements (S_1 and S_3 in the (0,1,-1) direction, S_2 and S_4 in the (0,-1,1) direction), the adatoms move normally to the surface and towards each other in a symmetric way. For Si-(2x2):B the atoms labelled 'S_i' are held fixed and the two adatoms form a symmetric dimer. The relevant displacements are given in table 7.3.

In table 7.4 are the total energies for the four (2x2) structures outlined in section 7.3.2. When calculating the total energies for the (2x1) structures, the atoms were fixed at their optimum position as quoted in table 7.2. Then from

Structure	Atom	Normal	In-plane	charge
Si-(2x2):A	S_i	0.02	0.20	-0.01
	A_i	0.57	0.22	0.02
Si-(2x2):B	S_i	-	-	0.06
	A_i	0.96	0.28	-0.12

Table 7.3: Normal and in-plane displacements for the two Si-(2x2) models, charge in atomic units.

Model	Total Energy
E_{A1}	-2359.5 eV
E_{A0}	-2354.1 eV
E_{B1}	-2342.4 eV
E_{B0}	-2327.9 eV

Table 7.4: The total energies in eV for each of the (2x2) models considered.

equation 7.3 we have:

$$\begin{aligned} E''_{A1} &= -2359.5 + \sum_{\text{bonds}}{}_{7} U_0 \\ E''_{A0} &= -2354.1 + \sum_{\text{bonds}}{}_{6} U_0 \\ E''_{B1} &= -2342.4 + \sum_{\text{bonds}}{}_{5} U_0 \\ E''_{B0} &= -2327.9 + \sum_{\text{bonds}}{}_{4} U_0. \end{aligned} \tag{7.4}$$

Then using Chadi's (1984) value of U_0,

$$\begin{aligned} E''_{A1} &= -2330.8 \text{ eV} \\ E''_{A0} &= -2329.5 \text{ eV} \\ E''_{B1} &= -2321.9 \text{ eV} \\ E''_{B0} &= -2311.5 \text{ eV}. \end{aligned} \tag{7.5}$$

7.4 Conclusions.

For the C-(2x1) structure, the result given in table 7.1 of a symmetric dimer seems acceptable as a possible model. For the Si-c(2x2) the very large charge transfer found and the non-existence of a dimer with lower charge transfer imply that a simple dimer model for the Si-c(2x2) structure is probably incorrect.

For the Si-(2x1) structure, equation 7.5 clearly shows that both adatom models prefer to form dimers (even though these (2x2) structures were not fully optimised) rather than stay in the (2x1) structure. Since no (2x2) structure has been observed experimentally, we conclude that the adatom models are incorrect for the (2x1) structure. This leaves the simple dimer as a possible model for the (2x1) structure, which could still be consistent with the reduction in the Si peak in the AES results (Dayan, 1986) when undergoing the transition Si-(2x1) → Si-c(2x2), if the Si-c(2x2) structure has only one Silicon atom per unit cell, this has also been

suggested by Kaplan (1988) based on experimental results.

There is clearly a need for more experimental work on the structure of this complex surface and particularly on the ratio of Silicon to Carbon in the surface layers if progress is to be made on the structure of the surfaces.

Chapter 8

Review and Further Work.

"If a man will begin with certainties, he shall end in doubts; but if he will be content to begin with doubts, he shall end in certainties."

— Francis Bacon, Advancement of Learning.

8.1 Review.

In chapters 2-5 I have been able to build upon the work of other authors in the use of Harrison's Empirical Tight-Binding Model to predict the behaviour of semiconductor surfaces using small atomic clusters.

Chapter 2.

I started with a review of the work that underpins the assumptions used within Harrison's model. I showed how by using a Linear Combination of Atomic Orbitals one can express the one-electron wave function of a polyatomic system. Then by using only the outermost $|S>$ and $|P>$ orbitals on an atom and restricting the

interactions to nearest-neighbour atoms, that one can construct a band structure for a crystal. The interatomic matrix elements, $V_{ss\sigma}$ etc., can then be used to "fit" the LCAO band structure to the bands determined by more accurate methods. Then I indicated how the interatomic matrix elements scaled from material to material according to a d^{-2} scaling rule. The chapter concludes by examining some of the work done in support of the model. This includes looking at which atomic orbitals need to be included, why only nearest-neighbour interactions are needed, the scaling rule required for the interatomic matrix elements so that they fit to a pressure dependent Hamiltonian and the orthogonality of the basis set.

Chapter 3.

Next came an examination of how to construct the total energy of a cluster of atoms, by using Chadi's total energy algorithm. This involves splitting the total energy into two parts, a sum over occupied states of one-electron energies and a residual energy. The one-electron energies are calculated within Harrison's Tight-Binding Model using the same parameter values as in the bulk. The residual energy is treated as a bond-stretching energy and is expanded as a polynomial about the appropriate equilibrium bond length. A different method, to that used by Chadi, is chosen to calculate the coefficients in the polynomial expansion. The method used fixes the coefficients of the bond stretching energy such that the total energy of a simple molecule, e.g. Si_2H_6, is correctly reproduced as the Si-Si bond length is varied. An accurate value of the total energy is obtained for the molecule by using a quantum chemistry package (GAMESS, Gaussian 82). The chapter concludes by examining how variations in the basis set used in the quantum chemistry package

affect the predictions of the model.

Chapter 4.

There then follows a consideration on how to systematically construct and enlarge clusters that mimic the behaviour of an infinite semiconductor surface. Any cluster that we wish to use needs to ensure that displaced atoms have the correct local bonding and that surface stoichiometry is maintained. It was also shown that the best way to deal with the pseudo-surfaces generated by the cluster was to saturate the dangling hybrids with hydrogen, rather than reduce the size of the basis set used to evaluate the one-electron energies. A method was also given to enlarge the clusters so that the local bonding was correct for moving atoms and the surface stoichiometry was maintained. This method could clearly be extended so that in the infinite limit the semi-infinite crystal would be produced. It was shown that the predictions made for the structures of semi-conductor surfaces converged very rapidly and that the minimal cluster in most cases gave acceptable answers.

Chapter 5.

This the last of the four chapters that deal with the construction of the model, considers what has been shown to be an important effect in tight-binding models. This is that the one-electron energies need to be calculated in a charge self-consistent manner. This was done by using a method introduced by Harrison to adjust the atomic term values. This method takes into account the excess charge on an atom and the Coulomb potential due to all the other atoms on the infinite surface. The difficulty with the method is that it is necessary to iterate the procedure, and

evaluate the one-electron energies up to sixty times for each geometry. This tends to make the calculations much longer. To overcome the problem of the increase in the length of calculations an ad hoc method was tried. This was to add a penalty function energy term which discriminated against those geometries which produced large charge transfers. The conclusion reached was that the charge discrimination model had in general multiple local minima, one of which was related to the non-self-consistent minimum and another to the self-consistent minimum. The charge discrimination model was therefore considered as an useful tool for estimating the minimum of the self-consistent problem. With the self-consistent model we agreed with Pandey that the Si(111) bulk terminated surface does not buckle; however, for the (1x1) structure no contraction of the surface layer was found. The structure predicted by the self-consistent model for the Si(100)(2x1) surface is highly buckled and has a large charge transfer, which is not in agreement with Pandey's prediction. For the GaAs(110)(1x1) surface I was unable to find a stable solution for the structure. However, since those calculations were performed, a problem with Harrison's charge self-consistent model has come to light. This will be discussed in section 8.2.

Chapters 6 and 7.

Chapters 6 and 7 use the tight-binding model to predict the structure found for a sub-monolayer coverage of Lead on a Germanium (111) substrate, and a sequence of different surface reconstructions found to occur on the (100) face of Cubic Silicon Carbide. For the Lead-Germanium system the adsorption site favoured by the self-consistent model is in agreement with that predicted by experimental work. There

is however, some disagreement over the exact position of some of the atoms within the unit cell. For the β-SiC(100) surface I was able to examine possible models for a number of different surface structures and to indicate which were the most likely to be found. However, further experimental work needs to be done on this surface before much can be said about the tight-binding results.

8.2 Further Work.

As was indicated in the last section there is a problem with Harrison's prescription (Harrison, 1985) for the charge self-consistency. It was pointed out in a paper by Harrison and Klepeis (1988) that if one uses Harrison's prescription for charge self-consistency within his Bond Orbital Model (Harrison, 1980, 1973), which is closely related to the model used in this thesis, that bulk Silicon "would be unstable against the formation of a charge density wave." This represents a serious failure of the model. Harrison concludes that the error is in assuming that the charges are spherically symmetric and non-overlapping (section 5.2). This suggests that the Coulomb potential(equation 5.1) needs to be adjusted in some way to remove the instability. Harrison however suggests that it is better to adjust the coefficient which relates to the intra-atomic Coulomb repulsion (W_s) in equation 5.1. He suggest that W_s for Silicon should be increased from 7.64 eV to 10.05 eV. There is clearly a need to examine this problem with care, since we know that introducing charge self-consistency is important.

A possible solution to the difficulty raised above, would be to include the self-consistency in a different way. Such a scheme has been suggested by Bechstedt

et al. (1985), who were also working within Harrison's tight-binding model. The advantage of adopting their scheme is that they calculate the residual energy in Chadi's total energy algorithm (equation 3.4) in a way that can also be treated within the self-consistency scheme, something that the model presented here does not do.

It would also be interesting to change the functional relationship of the inter-atomic matrix elements, $V_{ss\sigma}$ etc., so as to reflect changes in the pressure dependent band-structure of Silicon (Smith, 1986).

Working with the model as it stands, one could extend the self-consistency to more layers, and use the model to examine steps, point defects and possibly interfaces.

Appendix A

Sum of One-electron Energies within the Hartree-Fock Method.

Let us start with the antisymmetric wave function as developed by J.C. Slater (1960), known as the Slater determinant,

$$|\phi>=(N!)^{-1/2}\begin{vmatrix} U_\alpha(1) & \cdots & U_\alpha(N) \\ \vdots & & \vdots \\ U_\gamma(1) & \cdots & U_\gamma(N) \end{vmatrix} \tag{A.1}$$

where the $U_\lambda(i)$'s are spin orbitals. This may be written in the form,

$$|\phi>=(N!)^{-1/2}\sum_P(-1)^P P|\phi_H> \tag{A.2}$$

where

$$|\phi_H>=|U_\alpha(1)>|U_\beta(2)>\cdots|U_\gamma(N)>, \tag{A.3}$$

and P is an operator such that:

- $P(=0)$ leaves the wave function unchanged,
- $P(=1)$ produces all the permutations with two sets of electron coordinates interchanged,

- $P(=2)$ produces all the permutations with three sets of electron coordinates interchanged,
- etc...

i.e.

$$P(=0)|U_\alpha(1)>|U_\beta(2)>|U_\gamma(3)> = |U_\alpha(1)>|U_\beta(2)>|U_\gamma(3)>,$$

$$\begin{aligned} P(=1)|U_\alpha(1)>|U_\beta(2)>|U_\gamma(3)> &= |U_\alpha(1)>|U_\beta(3)>|U_\gamma(2)> \\ &+ |U_\alpha(3)>|U_\beta(2)>|U_\gamma(1)> \\ &+ |U_\alpha(2)>|U_\beta(1)>|U_\gamma(3)>, \end{aligned}$$

$$\begin{aligned} P(=2)|U_\alpha(1)>|U_\beta(2)>|U_\gamma(3)> &= |U_\alpha(2)>|U_\beta(3)>|U_\gamma(1)> \\ &+ |U_\alpha(3)>|U_\beta(1)>|U_\gamma(2)>. \end{aligned}$$

If we define

$$A = (N!)^{-1}\sum_P (-1)^p P, \tag{A.4}$$

$$\Rightarrow |\phi> = \sqrt{N!}A|\phi_H>. \tag{A.5}$$

Useful properties of the operator A are;

$$A^2 = A \quad , \quad [H_1, A] = [H_2, A] = 0, \tag{A.6}$$

H_1 and H_2 being the one and two electron operators defined below,

$$H_1 = \sum_i h_i \qquad h_i = -\frac{1}{2}\nabla_i^2 - \frac{Z}{r_i} \tag{A.7}$$

$$H_2 = \sum_{i<j} \frac{1}{r_{ij}} \qquad r_{ij} = |r_i - r_j|. \tag{A.8}$$

If E_{HF} is the energy of the system, then

$$\begin{aligned} E_{HF} &= <\phi|H_1|\phi> &&+ <\phi|H_2|\phi> \\ &= N! <\phi_H|AH_1A|\phi_H> &&+N! <\phi_H|AH_2A|\phi_H> \\ &= N! <\phi_H|H_1A^2|\phi_H> &&+N! <\phi_H|H_2A^2|\phi_H> \\ &= N! <\phi_H|H_1A|\phi_H> &&+N! <\phi_H|H_2A|\phi_H> . \end{aligned} \tag{A.9}$$

Consider the first term,

$$<\phi|H_1|\phi> = \sum_i \sum_P (-1)^P <\phi_H|\hat{h}_i P|\phi_H>, \tag{A.10}$$

then for some fixed 'i', we have

$P(=0)$

$$<U_\gamma(N)|\cdots<U_\zeta(i)|\cdots<U_\beta(2)|<U_\alpha(1)|\hat{h}_i|U_\alpha(1)>|U_\beta(2)>\cdots|U_\zeta(i)>\cdots|U_\gamma(N)>, \tag{A.11}$$

pulling terms through gives

$$\underset{=1}{<U_\alpha(1)|U_\alpha(1)>}\ \underset{=1}{<U_\beta(2)|U_\beta(2)>}\ \cdots\ <U_\zeta(i)|\hat{h}_i|U_\zeta(i)>\ \cdots\ \underset{=1}{<U_\gamma(N)|U_\gamma(N)>} \tag{A.12}$$

$$\Rightarrow <U_\zeta(i)|\hat{h}_i|U_\zeta(i)>, \tag{A.13}$$

$P(=1)$, operating just on the ith and jth electrons

$$-<U_\gamma(N)|\cdots<U_\lambda(j)|\cdots<U_\zeta(i)|\cdots<U_\alpha(1)|\hat{h}_i|U_\alpha(1)>\cdots|U_\zeta(j)>\cdots|U_\lambda(i)>\cdots|U_\gamma(N)>, \tag{A.14}$$

pulling terms through gives

$$\underset{=1}{<U_\alpha(1)|U_\alpha(1)>}\ \cdots\ \underset{=0}{<U_\zeta(i)|U_\zeta(j)>}\ \cdots\ <U_\lambda(j)|\hat{h}_i|U_\lambda(i)>\ \cdots\ \underset{=1}{<U_\gamma(N)|U_\gamma(N)>}, \tag{A.15}$$

hence it gives no contribution, the same holds true for higher orders of P. Summing equation A.13 over 'i' is equivalent to summing over 'ζ', hence

$$< \phi|H_1|\phi >= \sum_{\zeta} < U_\zeta(1)|\hat{h}_1|U_\zeta(1) > . \tag{A.16}$$

Taking the second term

$$< \phi|H_2|\phi >= \sum_{i<j} \sum_{P} (-1)^P < \phi_H|\frac{1}{r_{ij}}P|\phi_H >, \tag{A.17}$$

then for fixed 'i' and 'j'

$P(=0)$ gives

$$< U_\lambda(i)| < U_\mu(j)|\frac{1}{r_{ij}}|U_\mu(j) > |U_\lambda(i) >, \tag{A.18}$$

$P(=1)$ gives

$$- < U_\lambda(i)| < U_\mu(j)|\frac{1}{r_{ij}}|U_\mu(i) > |U_\lambda(j) >, \tag{A.19}$$

$P(\geq 2)$ gives zero as before.

Then we have

$$< U_\lambda(i)| < U_\mu(j)|\frac{1}{r_{ij}}|U_\mu(j) > |U_\lambda(i) > - < U_\lambda(i)| < U_\mu(j)|\frac{1}{r_{ij}}|U_\mu(i) > |U_\lambda(j) >, \tag{A.20}$$

replacing the $\sum_{i<j}$ by $\sum_{\lambda<\mu}$, we get

$$< \phi|H_2|\phi >= \sum_{\lambda<\mu} < U_\mu(1)U_\lambda(2)|\frac{1}{r_{12}}(|U_\mu(1)U_\lambda(2) > -|U_\mu(2)U_\lambda(1) >). \tag{A.21}$$

Equation A.9 can now be written in the form

$$\begin{aligned} E_{HF} &= \sum_{\zeta} < U_\zeta(1)|\hat{h}_1|U_\zeta(1) > \\ &+ \sum_{\lambda<\mu} < U_\mu(1)U_\lambda(2)|\frac{1}{r_{12}}(|U_\mu(1)U_\lambda(2) > -|U_\mu(2)U_\lambda(1) >), \end{aligned} \tag{A.22}$$

converting to double sums

$$\begin{aligned} E_{HF} &= \sum_{\zeta} < U_\zeta(1)|\hat{h}_1|U_\zeta(1) > \\ &+ \frac{1}{2}\sum_{\lambda\mu} < U_\mu(1)U_\lambda(2)|\frac{1}{r_{12}}(|U_\mu(1)U_\lambda(2) > -|U_\mu(2)U_\lambda(1) >). \end{aligned} \tag{A.23}$$

The next step is to use the method of undetermined multipliers to vary one of the spin orbitals, U_i, while preserving its normalisation and orthogonality. We demand that E_{HF} be stationary for this variation. Hence

$$\delta\{E_{HF} - \sum_i \epsilon_{iHF} < U_i(1)|U_i(1) >\} = 0, \tag{A.24}$$

with ϵ_{iHF} being an undetermined multiplier,

$$\sum_i < \delta U_i(1)|\{\hat{h}_1 + \sum_j < U_j|\frac{1}{r_{12}}|U_j(2) > - \frac{\sum_j <U_i(1)U_j(2)|1/r_{12}|U_i(2)U_j(1)>}{<U_i(1)|U_i(1)>} - \epsilon_{iHF}\}|U_i(1) > + \text{complex conjugate} = 0. \tag{A.25}$$

This holds true for arbitrary $< \delta U_i(1)|$ only if

$$\hat{h}_1|U_i(1) > + \sum_j < U_j(2)|\frac{1}{r_{12}}|U_j(2) > |U_i(1) > - \sum_j < U_i(1)U_j(2)|\frac{1}{r_{12}}|U_i(2)U_j(1) > |U_i(1) > = \epsilon_{iHF}|U_i(1) > . \tag{A.26}$$

Pre-multiplying by $< U_i(1)|$ and summing over 'i', gives

$$\sum_i \epsilon_{iHF} = \sum_i < U_i(1)|\hat{h}_1|U_i(1) > + \sum_{ij} < U_i(1)U_j(2)|\frac{1}{r_{12}}\{|U_i(1)U_j(2) > - |U_i(2)U_j(1) >\}. \tag{A.27}$$

If we write $< \phi|H_1|\phi >= E_{KE} + E_{ne}$, where

- E_{KE} is the Kinetic Energy of the system,
- E_{ne} is the ion-electron interaction energy,

and $< \phi|H_2|\phi >= E_{ee}$

- E_{ee} is the electron-electron interaction energy.

Then equation A.23 can be written as

$$E_{HF} = E_{KE} + E_{ne} + E_{ee}. \tag{A.28}$$

By comparing equations A.23 and A.27,

$$\sum_i \epsilon_{iHF} = E_{KE} + E_{ne} + 2E_{ee}, \tag{A.29}$$

where ϵ_{iHF} is a one-electron energy eigenvalue.

Appendix B

Coefficients for the Bond Stretching Energy.

Given here are the coefficients for the bond-stretching energy (equation 3.5) for all of the bonds that I have worked with. The equilibrium bond length (d_0) about which the polynomial expansion was carried out and the range of bond lengths for which the coefficients hold are also given.

bond	Si-Si	Ga-As	Si-C	C-C
d_0	2.3516 Å	2.45 Å	1.88 Å	1.54 Å
range	2.0-3.0 Å	2.0-3.0 Å	1.5-2.5 Å	1.0-2.0 Å
U_1	-23.594186	-20.014700	-37.509908	-57.260914
U_2	65.607786	44.899478	89.764924	124.674452
U_3	-123.577104	-82.851358	-151.117230	-204.700037
U_4	180.800068	67.746153	209.553458	274.731552
U_5	-170.202240	-147.696942	-271.140378	-283.539484
U_6	245.761514	202.335372	368.805479	460.588144
U_7	-593.660664	-283.214224	-354.397705	-958.300808

bond	Ge-Ge	Ge-Pb	Si-O
d_0	2.44 Å	2.84 Å	1.64 Å
range	2.0-3.0 Å	2.0-3.5 Å	1.1-2.6 Å
U_1	-17.632699	-15.171545	-94.350810
U_2	54.482799	56.838678	255.688650
U_3	-103.506279	-124.532906	-493.620807
U_4	150.318973	201.664854	802.938032
U_5	-183.229900	-254.061283	-1448.099910
U_6	236.196654	447.359560	2172.025980
U_7	-425.734599	-900.031592	-1411.434997

Bibliography

[1] Anderson D.G., (1965), J. Assoc. Comp. Mach. 12, 547.

[2] Appelbaum J.A., Hamann D.R., (1976), Phys. Rev. Letts. 36, 168.

[3] Barone V., Lelj F., Russo N., Toscano M., (1985), Surf. Sci. 162, 230.

[4] Barone V. (1987) Surf. Sci. 189/90, 106.

[5] Batra I.P., Ciraci S., (1975), Phys. Rev. Letts. 34, 1337.

[6] Batra I.P., Ciraci S., Ortenburger I.B., (1976a), Sol. Stat. Comm. 18, 563.

[7] Batra I.P., Ciraci S., (1976b), Phys. Rev. Letts. 36, 170.

[8] Bechstedt F., Reichardt D., Enderlein R., (1985), Phys. Stat. Sol. b 131, 643.

[9] Bloch F. (1928), Z. Physik 52, 555.

[10] Chadi D.J., Cohen M.L., (1975), Phy. Stat. Sol. b 68, 405.

[11] Chadi D.J., (1977), Phys. Rev. B 16, 3572.

[12] Chadi D.J., (1978), Phys. Rev. Lett. 41, 1062.

[13] Chadi D.J., (1979), Phys. Rev. Letts. 43, 43.

[14] Chadi D.J., (1983), Vacuum 33, 613.

[15] Chadi D.J., (1984), Phys. Rev. B 29, 785.

[16] Chelikowsky J.R., Cohen M.L. (1976), Phys. Rev. B 14, 556.

[17] Cohen M.L., Bergstresser T.K., (1966), Phys. Rev. 141. 789.

[18] Dayan M., (1985), J. Vac. Sci. Tech. A 3, 361.

[19] Dayan M., (1986), J. Vac. Sci. Tech. A 4, 38.

[20] Dederichs P.H., Zeller R., (1983), Phys. Rev. B 28, 5462.

[21] Feidenhans'l R., Pedersen J.S., Nielsen M., Grey F. Johnson R.L., (1986), Surf. Sci. 178, 927.

[22] Froyen S., Harrison W.A., (1979), Phys. Rev. B 20, 2420.

[23] GAMESS

- Dupuis M., Spangler D., Wendoloski J., NRCC Software Catalog, Volume 1 Program number QG01 (GAMESS), 1980.
- Guest M.F., Kendrick J., Pope S.A., GAMESS User Manual, SERC Daresbury Laboratory, DL/SCI,TM000T, 1984.

[24] Gaussian 82, Carnegie Mellon University (Vendor of Licence).

[25] Gill P.E., Murray W., (1978), J. Numerical Analy. 15, 977.

[26] Grobman W.D., Eastman D.E., Freeouf J.L., (1975), Phy. Rev. B 12, 4405.

[27] Harrison W.A., (1973), Phys. Rev. B 8, 4487.

[28] Harrison W.A., (1977), Festkörperprobleme, Editor: Treusch J., Vol XVII, p. 135, Publisher: Vieweg Braunschweig.

[29] Harrison W.A., (1980), Electronic Structure and the Properties of Solids, Publisher: W.H. Freeman and Company.

[30] Harrison W.A., (1984), Proceedings of the 17th International Conference on the Physics of Semiconductors, p.989., Editors: Chadi D.J., Harrison W.A., Publisher: Springer-Verlag.

[31] Harrison W.A., (1985), Phys. Rev. B 31, 2121.

[32] Harrison W.A., Klepeis J.E., (1988), Phys. Rev. B 37, 864.

[33] Huzinaga S., (1984), Gaussian Basis Sets for Molecular Calculations, Publisher: Elsevier Science Publishers.

[34] Ichikawa T., (1983), Sol. Stat. Comm. 46, 827.

[35] Kaplan R., Parrill T.M., (1986), Surf. Sci. 165, L45.

[36] Kaplan R., (1988), J. Vac. Sci. Tech. A 6, 829.

[37] Keating P.N., (1966), Phys. Rev. 145, 637.

[38] Kittel C., (1976), Introduction to Solid State Physics, 5th Edition, Publishers: John Wiley and Sons.

[39] Le Lay G., Metóis J.J., (1983), Appl. Surf. Sci. 17, 131.

[40] Le Lay G., Metóis J.J., (1984), J. de Phy. C5, 427.

[41] Li M., Tonner B.P. (1988), Surf. Sci. 193, 10.

[42] Löwdin P.O., (1950), J. Chem. Phys. 18, 365.

[43] Mailhoit C., Duke C.B., Chadi D.J., (1985), Phys. Rev. B 31, 2215.

[44] Messner R.P., (1979), The Nature of the Surface Chemical Bond, Editors: Rhodin T.N., Ertl G., Publishers: North-Holland Publishing Company.

[45] NAG-Numerical Algorithms Group, version 12, routine E04FDF.

[46] Nichols J.M., Martensson P., Hansson G.V., Northup J.E., (1985), Phys. Rev. B 32, 1333.

[47] Nishida M., (1978), Surf. Sci. 72, 589.

[48] Nishino S., Powell J.A., Will H.A. (1983), Appl. Phys. Lett. 42, 460.

[49] Northup J.E., (1984), Phys. Rev. Letts. 53, 683.

[50] Pandey K.C., (1982), Phys. Rev. Letts. 49, 223.

[51] Pantelides S.T., Harrison W.A., (1975), Phys. Rev. B 11, 3006.

[52] Pantelides S.T., Harrison W.A.. (1976), Phys. Rev. B 13, 2667.

[53] Pantelides S.T., Pollman J., (1979), J. Vac. Sci. Tech. 16, 1349.

[54] Pederson J.S., Feidenhans'l R., Nielsen M., Kjœrk K., Grey F., Johnson R.L., (1987), Surf. Sci. 189, 1047.

[55] Pedersen J.S., (1988), An X-ray Diffraction Study of the Reconstructions Induced by Sn and Pb on Ge(111) Surfaces. Ph.D. Thesis Risø National Laboratory. DK-4000, Roskilde Denmark.

[56] PHYS/PG3, Preparation of Ph.D. Thesis, Department of Physics, University of Warwick, June 1988.

[57] Redondo A., Goddard W.A. III, McGill T.C., Surratt G.T., (1977), Sol. Stat. Comm. 21, 991.

[58] Robertson J., (1983), Phil. Mag. B 47, L33.

[59] Sano N., Kato H., Nakayama M., Chika S., Terauchi H., (1984), Jap. J. Appl. Phys. 23, L640.

[60] Slater J.C., Koster G.F., (1954), Phys. Rev. 94, 1498.

[61] Slater J.C., (1960), Quantum Theory of Atomic Structure, Vol. 1 Chapter 12, Publishers: McGraw Hill Book Company.

[62] Smith P.V., McMahon D., (1983), J. Phys. C 16, 6947.

[63] Smith P.V., (1985), Appl. of Surf. Sci., 22/23, 596.

[64] Smith P.V., (1986), J. Phys Chem. Solids 47, 147.

[65] Swarts C.A., McGill T.C., Goddard W.A. III, (1981), Surf. Sci. 110, 400.

[66] Takai T, Halicioglu T., Tiller W.A, (1985), Surf. Sci. 164, 341.

[67] Tománek D., Schlüter M.A., (1986), Phys. Rev. Letts. 56, 1055.

[68] Tromp R.M., Homers R.J., Demuth J.E., (1985), Phys. Rev. Letts. 55, 1303.

[69] Watkins G.D., Messmer R.P., (1974), Phys. Rev. Letts. 32, 1244.

[70] Woodruff D.P., Delchar T.A., (1986), Modern Techniques of Surface Science, Publisher: Cambridge University Press.

[71] Zangwill A., (1988), Physics at Surfaces, Publisher: Cambridge University Press.

[72] Ziman J.M., (1963), Principles of the Theory of Solids, 2nd edition, p.39, Publishers: Cambridge University Press.

"Everything in this book may be wrong."

— Richard Bach, Illusions.